MICE

Cosmological Simulations @
Marenostrum Supercomputer
using 4000 processors

nonlinear clustering
from theory and numerical simulations

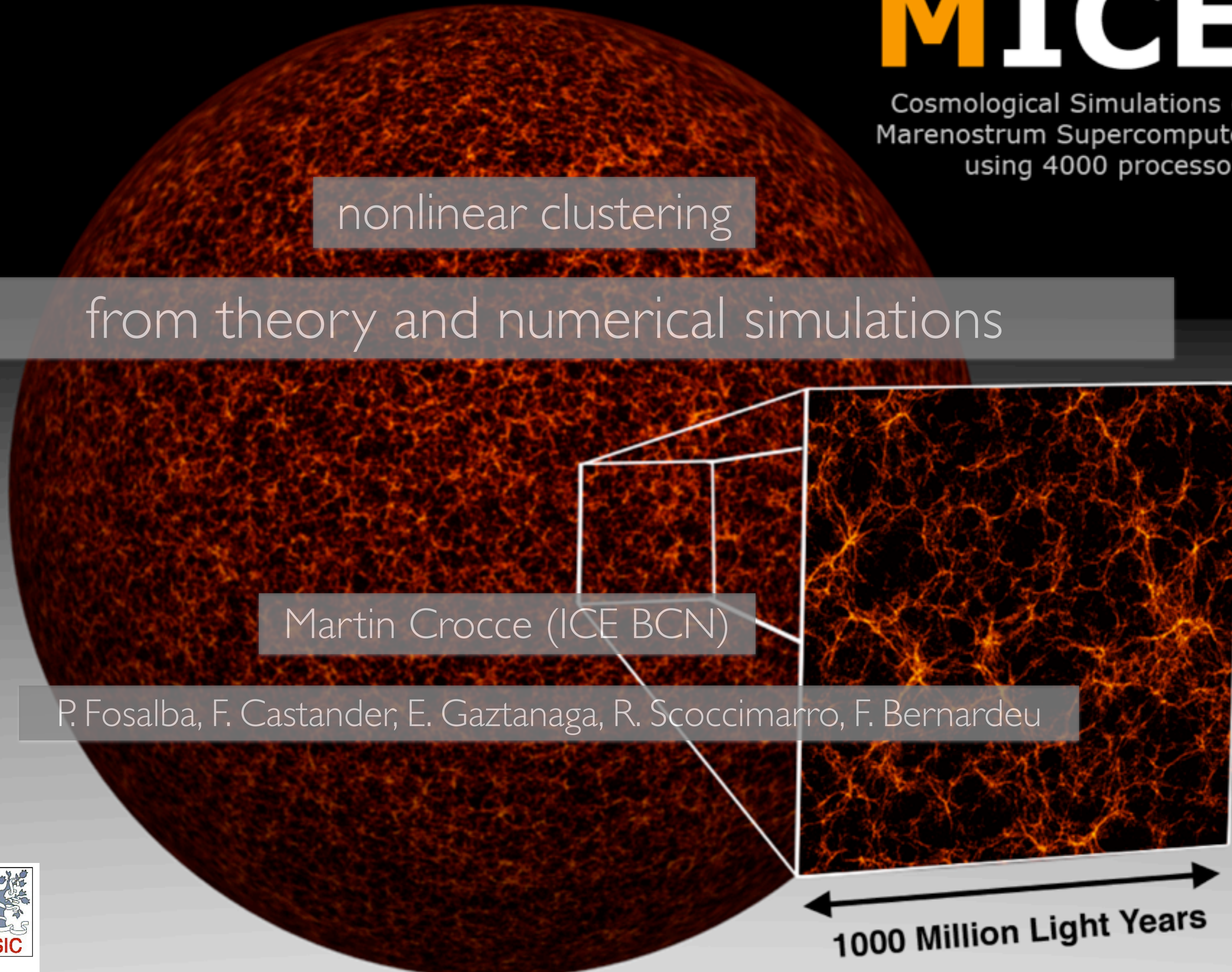

Martin Crocce (ICE BCN)

P. Fosalba, F. Castander, E. Gaztanaga, R. Scoccimarro, F. Bernardeu

INSTITUT D'ESTUDIS ESPACIALS DE CATALUNYA
IEEC
CSIC
ICE

Motivation

Given ongoing and near future very large datasets (lss, lensing, clusters,..) how do we extract the most out of them

For LSS at smaller scales S/N is much better but we have to deal with nonlinearities (not that trivial for PT)

A complementary approach is to use simulations (in particular for smaller scales related to weak lensing)

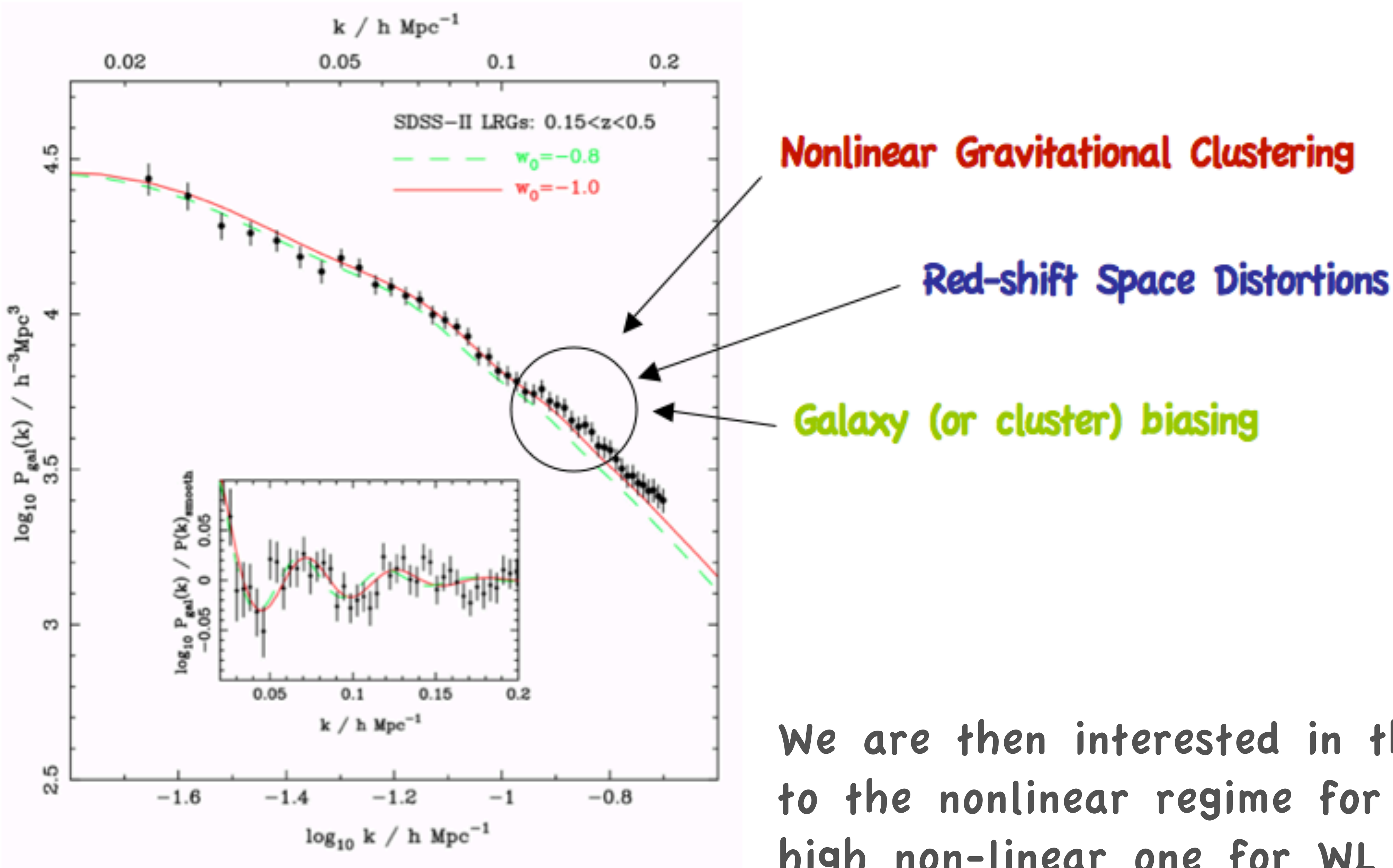

We are then interested in the transition to the nonlinear regime for LSS and the high non-linear one for WL

Outline

- Nonlinear gravitational clustering & Perturbation Theory
  Renormalized Perturbation Theory
  Performance of approaches, requirements from parameter estimate (code performance)

- Simulations
  Introduce some of the state-of-the-art runs : MICE-GC run

- Limitations of N-bodies, things we want to keep in mind

- Mass Resolution Effects in clustering for LSS and lensing

- MICE public light-cone galaxy mock catalogue

Nonlinear Gravitational Clustering

scales much smaller than the Horizon (Hubble radius) $\longrightarrow$ Newtonian gravity

scales larger than strong clustering regime $\longrightarrow$ *single stream approximation*

no velocity dispersion or pressure
(prior to virialization and shell crossing)

$$\nabla^2\Phi(\mathbf{x},\tau) = \frac{3}{2}\Omega_m(\tau)\ \mathcal{H}^2(\tau)\ \delta(\mathbf{x},\tau)$$

$$\frac{\partial\delta(\mathbf{x},\tau)}{\partial\tau} + \nabla\cdot\{[1+\delta(\mathbf{x},\tau)]\,\mathbf{u}(\mathbf{x},\tau)\} = 0$$

$$\frac{\partial\mathbf{u}(\mathbf{x},\tau)}{\partial\tau} + \mathcal{H}(\tau)\ \mathbf{u}(\mathbf{x},\tau) + \mathbf{u}(\mathbf{x},\tau)\cdot\nabla\mathbf{u}(\mathbf{x},\tau) = -\nabla\Phi(\mathbf{x},\tau)$$

velocity field can be assumed irrotational $\quad \theta(\mathbf{x},\tau)\ \equiv\ \nabla\cdot\mathbf{u}(\mathbf{x},\tau)$

$$\frac{\partial\tilde{\delta}(\mathbf{k},\tau)}{\partial\tau} + \tilde{\theta}(\mathbf{k},\tau) = -\int d^3k_1 d^3k_2\, \delta_{\rm D}(\mathbf{k}-\mathbf{k}_1-\mathbf{k}_2)\, \alpha(\mathbf{k}_1,\mathbf{k}_2)\, \tilde{\theta}(\mathbf{k}_1,\tau)\, \tilde{\delta}(\mathbf{k}_2,\tau),$$

$$\frac{\partial\tilde{\theta}(\mathbf{k},\tau)}{\partial\tau} + \mathcal{H}(\tau)\tilde{\theta}(\mathbf{k},\tau) + \frac{3}{2}\Omega_m(\tau)\mathcal{H}^2(\tau)\tilde{\delta}(\mathbf{k},\tau) = -\int d^3k_1 d^3k_2\, \delta_{\rm D}(\mathbf{k}-\mathbf{k}_1-\mathbf{k}_2)\beta(\mathbf{k}_1,\mathbf{k}_2)\, \tilde{\theta}(\mathbf{k}_1,\tau)\, \tilde{\theta}(\mathbf{k}_2,\tau)$$

Linear order $\delta_L(k,z) = D_+(z)\delta_0(k) \xrightarrow[\langle\delta(\mathbf{k})\delta(-\mathbf{k})\rangle]{} P_{\rm lin}(k,z) = [D_+(z)]^2 P_0(k)$.

Standard perturbation theory expands the density contrast in terms of the linear solution,

$$P(k,z) = D_+^2(z)P_0(k) + \underbrace{P_{13}(k,z) + P_{22}(k,z)}_{\text{1 - loop terms}} + \ldots$$

$$P_{22}(k,\tau) \equiv 2\int [F_2^{(s)}(\mathbf{k}-\mathbf{q},\mathbf{q})]^2 P_L(|\mathbf{k}-\mathbf{q}|,\tau)P_L(q,\tau)\mathrm{d}^3\mathbf{q},$$

$$P_{13}(k,z) \equiv D_+^2(z)P_0(k)6\int \mathrm{F}_3^{(s)}(\mathbf{k},\mathbf{q},-\mathbf{q})P_{\rm lin}(q,z)d^3\mathbf{q}$$

This expansion is valid at large scales where fluctuations are small, but it brakes down when approaching the nonlinear regime where $\Delta_{\rm lin} \gtrsim 1$.

Way out is to sum up all orders (!)

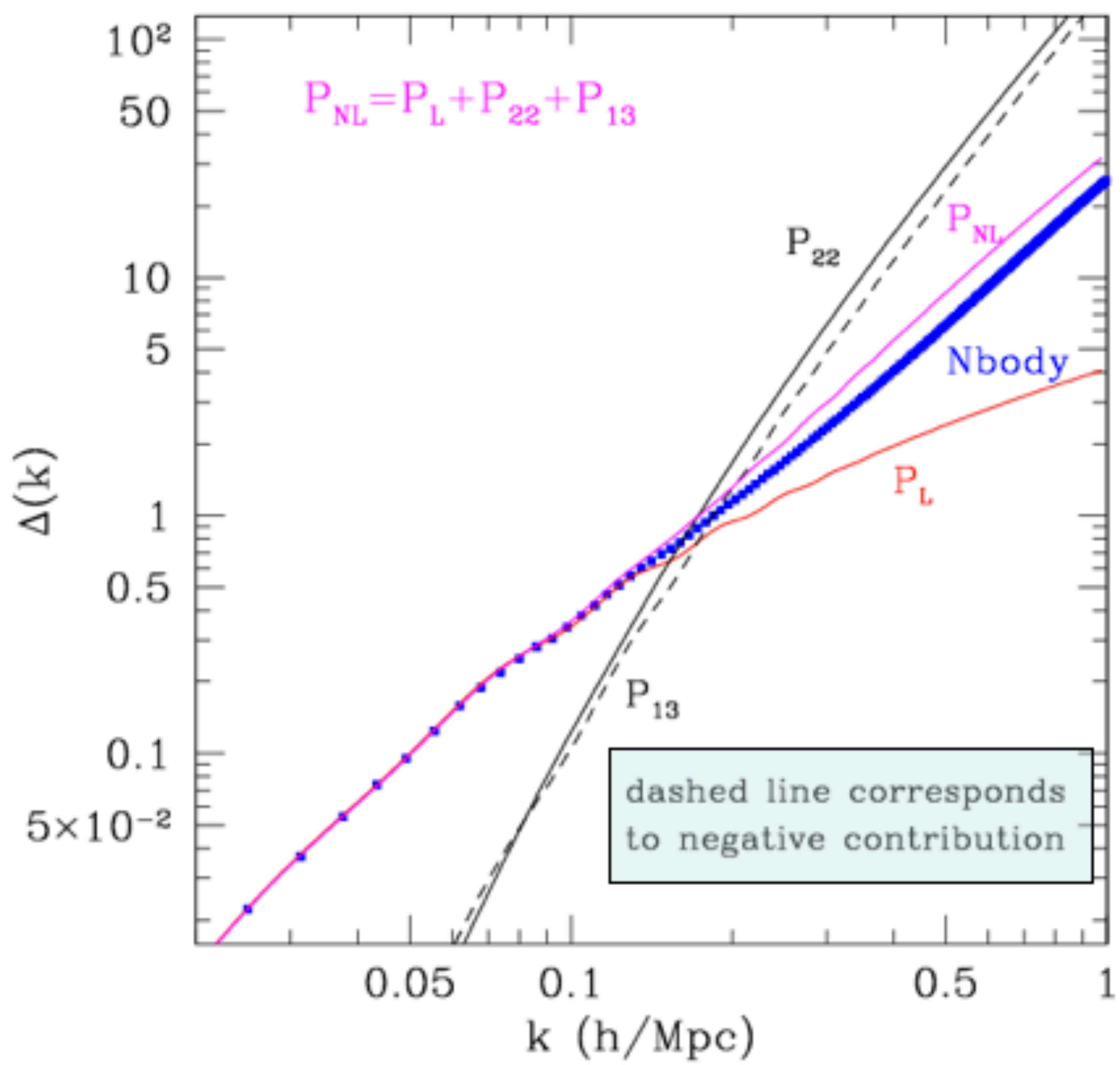

Power spectrum

$$\langle \Psi(k,a)\Psi(-k,a)\rangle$$

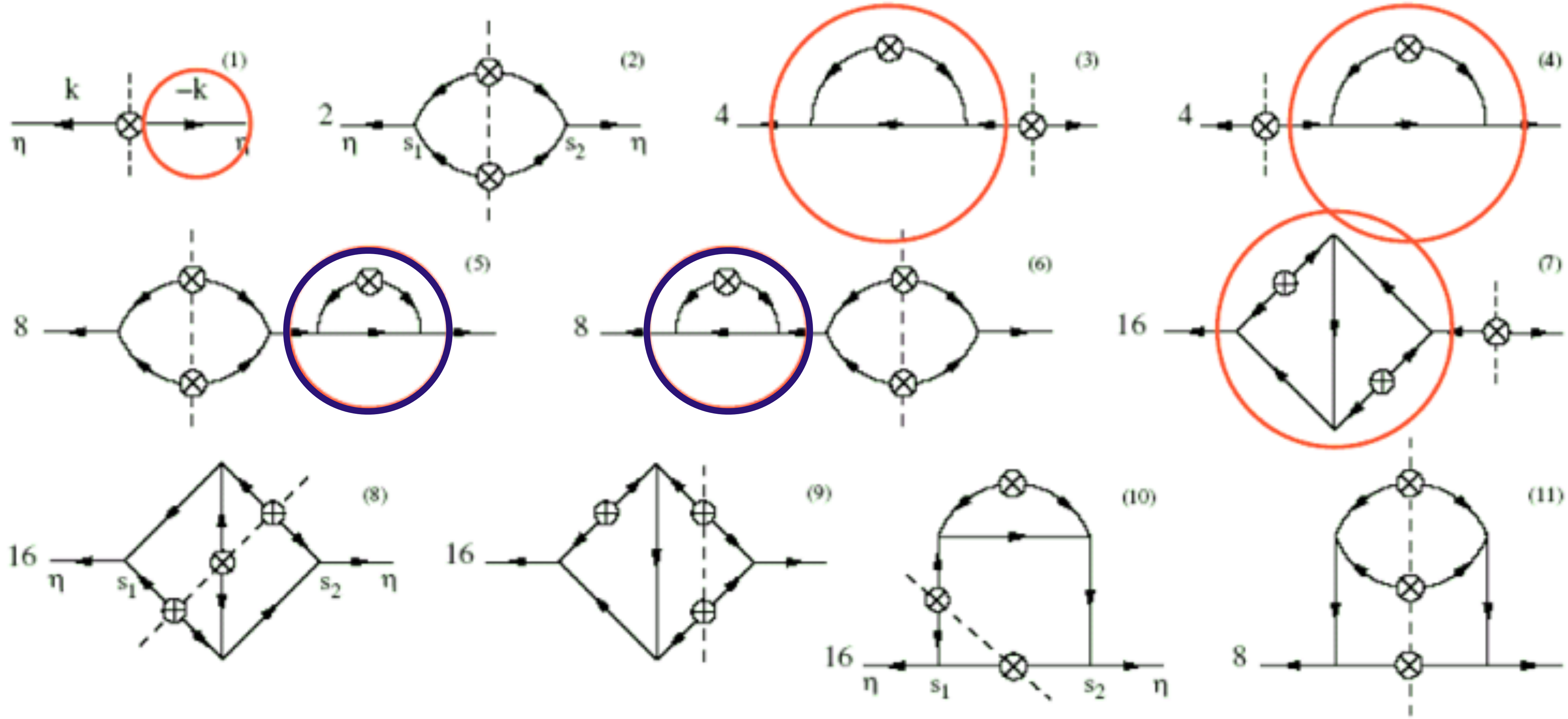

all orders can be systematically incorporated

Nonlinear Propagator

(Crocce & Scocimarro 2006)

$$G(k,\eta) \equiv \left\langle \frac{\delta \Psi_a(\mathbf{k},\eta)}{\delta \phi_b(\mathbf{k}')} \right\rangle =$$

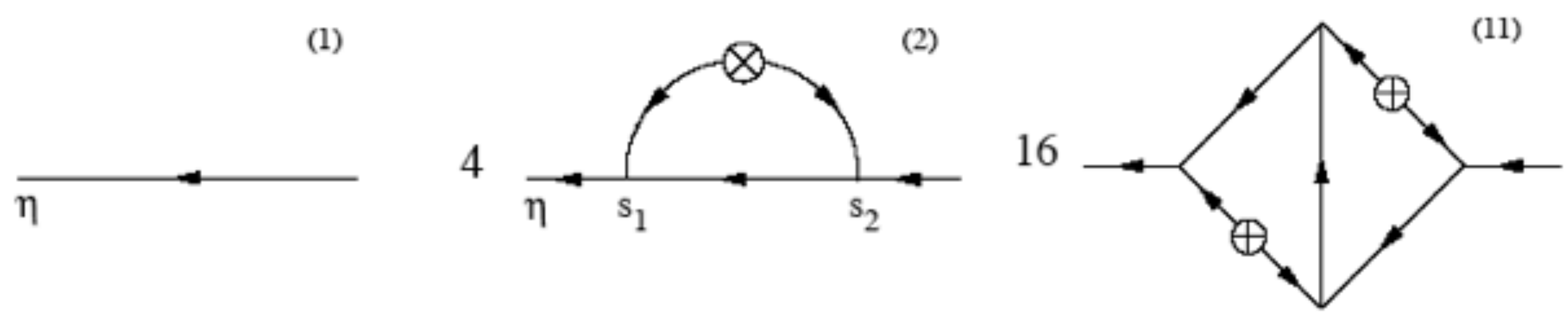

The Power Spectrum in RPT

$$P(k,z) = G_\delta^2(k,z) \times P_{\mathrm{Linear}}(k) + P_{\mathrm{ModeCoupling}}(k,z)$$

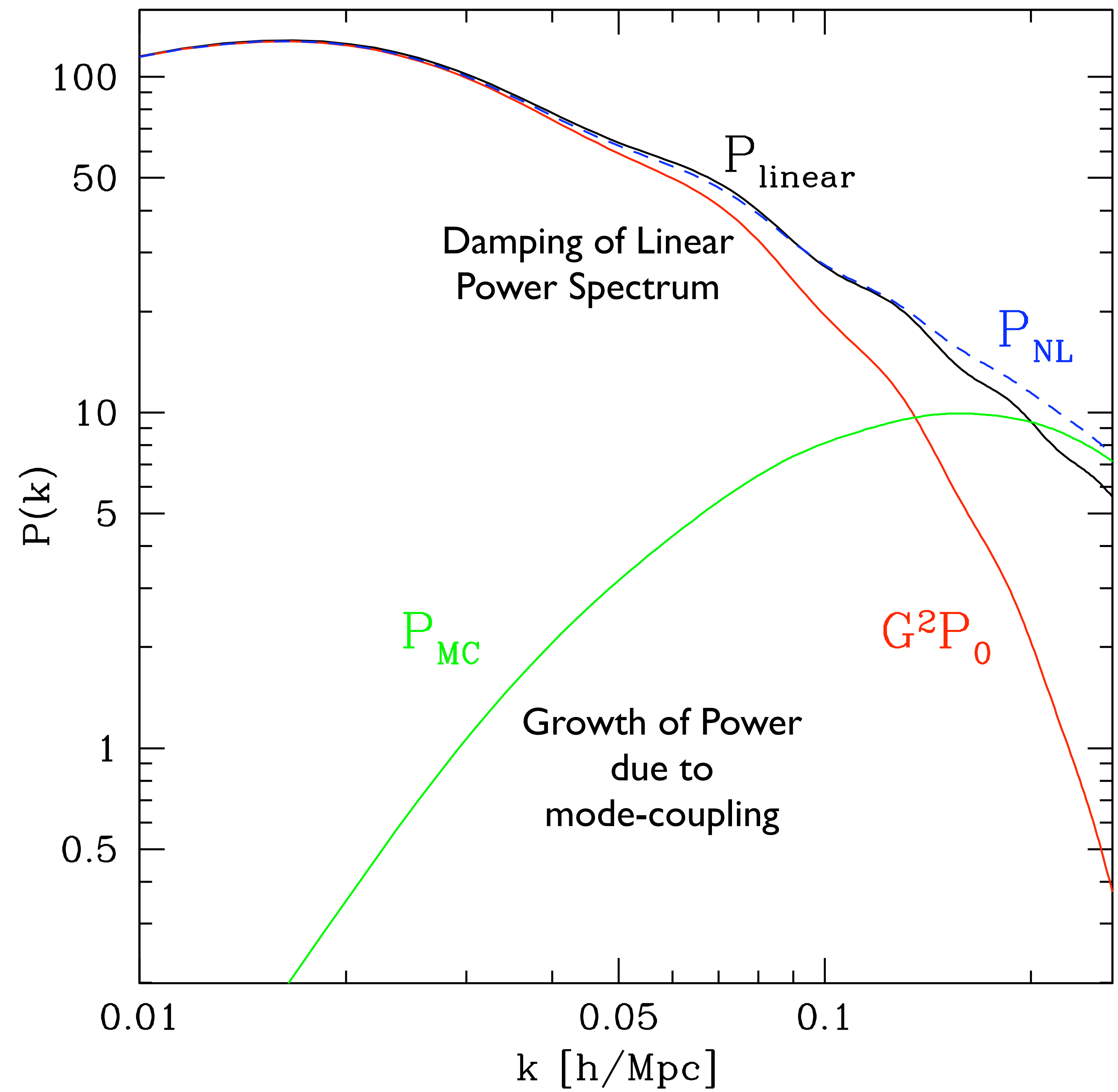

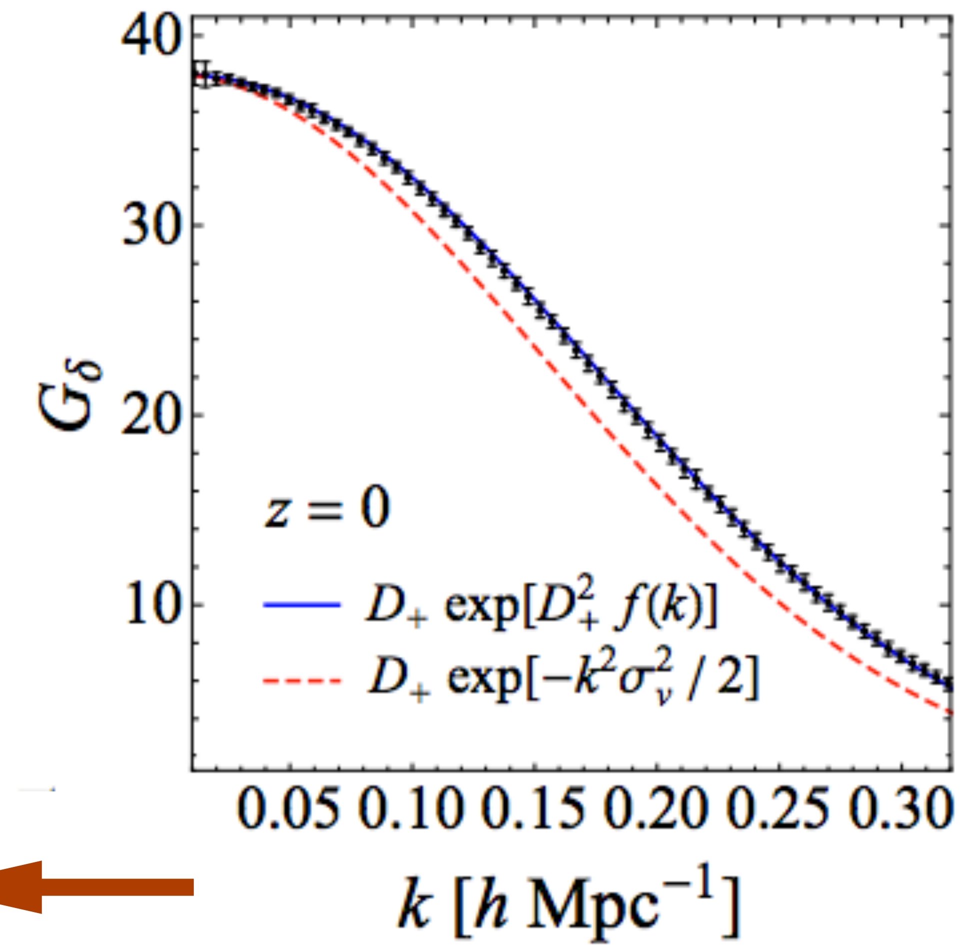

It is possible to re-organize the series by re-summing (infite) terms.
A new set of object appears,
(bernardeau crocce & sccocimarro 2008)

final den or vel field

$$\delta_{\rm D}(\mathbf{k}-\mathbf{k}_{1\ldots p})\,\Gamma^{(p)}_{ab_1\ldots b_p}(\mathbf{k}_1,\ldots,\mathbf{k}_p)=\frac{1}{p!}\left\langle\frac{\partial^p\Psi_a(\mathbf{k})}{\partial\Phi_{b_1}(\mathbf{k}_1)\ldots\partial\Phi_{b_p}(\mathbf{k}_p)}\right\rangle$$

initial field

✓ Natural extension of the RPT propagator : $G_{ab}(k,\eta)\;\delta_{\rm D}(\mathbf{k}-\mathbf{k}')\equiv\left\langle\frac{\delta\Psi_a(\mathbf{k},\eta)}{\delta\phi_b(\mathbf{k}')}\right\rangle$

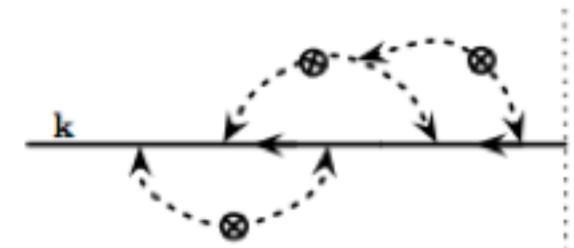

✓ "Renormalization" of the PT kernels :

$$\Gamma^{(n)}(\mathbf{q}_1,\cdots,\mathbf{q}_n)=\mathrm{F}^{(n)}(\mathbf{q}_1,\cdots,\mathbf{q}_n)+\text{“nonlinear corrections”}$$

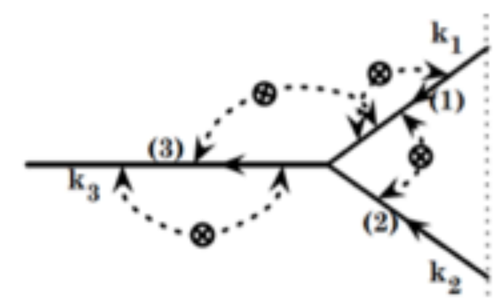

✓ They satisfy :

$$\delta_{\rm D}(\mathbf{k}-\mathbf{q}_{1\ldots p})\Gamma^{(n)}(\mathbf{q}_1,\cdots,\mathbf{q}_n)\;\begin{cases}\delta_{\rm D}[.]\;\mathrm{F}^{(n)}(\mathbf{q}_1,\cdots,\mathbf{q}_n) & \text{for low } k\\ \boxed{\delta_{\rm D}[.]\;\exp\left(-k^2\sigma_v^2/2\right)\mathrm{F}^{(n)}(\mathbf{q}_1,\cdots,\mathbf{q}_n)\quad \text{for high } k} & \\ \sim\langle\Psi(\mathbf{k})\Phi(-\mathbf{q}_1)\ldots\Phi(-\mathbf{q}_p)\rangle & \end{cases}$$

$$\sigma_v^2=\frac{1}{3}\int_0^\infty\frac{d^3\mathbf{k}}{k^2}P_{\rm Lin}(k)$$

Reconstruction of P(k) from Multi-point propagators

$$P_{ab}(\mathbf{k},\eta) = \sum_t t! \int \mathrm{d}^3\mathbf{q}_1 \ldots \mathrm{d}^3\mathbf{q}_t \,\delta_\mathrm{D}(\mathbf{k}-\mathbf{q}_{1\ldots t})\,\Gamma_a^{(t)}(\mathbf{q}_1,\ldots,\mathbf{q}_t;\eta)\,\Gamma_b^{(t)}(\mathbf{q}_1,\ldots,\mathbf{q}_t;\eta)\,P_0(q_1)\ldots P_0(q_t),$$

- **Sum of positive contributions**

$$P_{\delta\delta}(k) = \left[\Gamma_\delta^{(1)}(k,z)\right]^2 P_0(k) + 2\int d^3q \left[\Gamma_\delta^{(2)}(\mathbf{k}-\mathbf{q},\mathbf{q},z)\right]^2 P_0(|\mathbf{k}-\mathbf{q}|)P_0(q) + \ldots$$

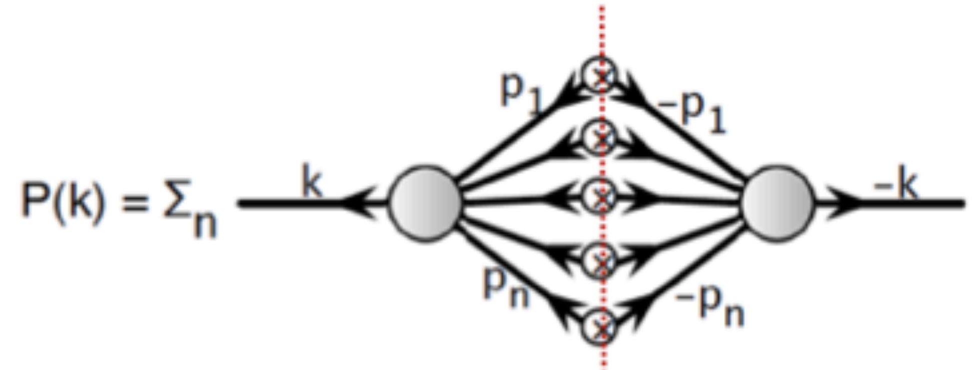

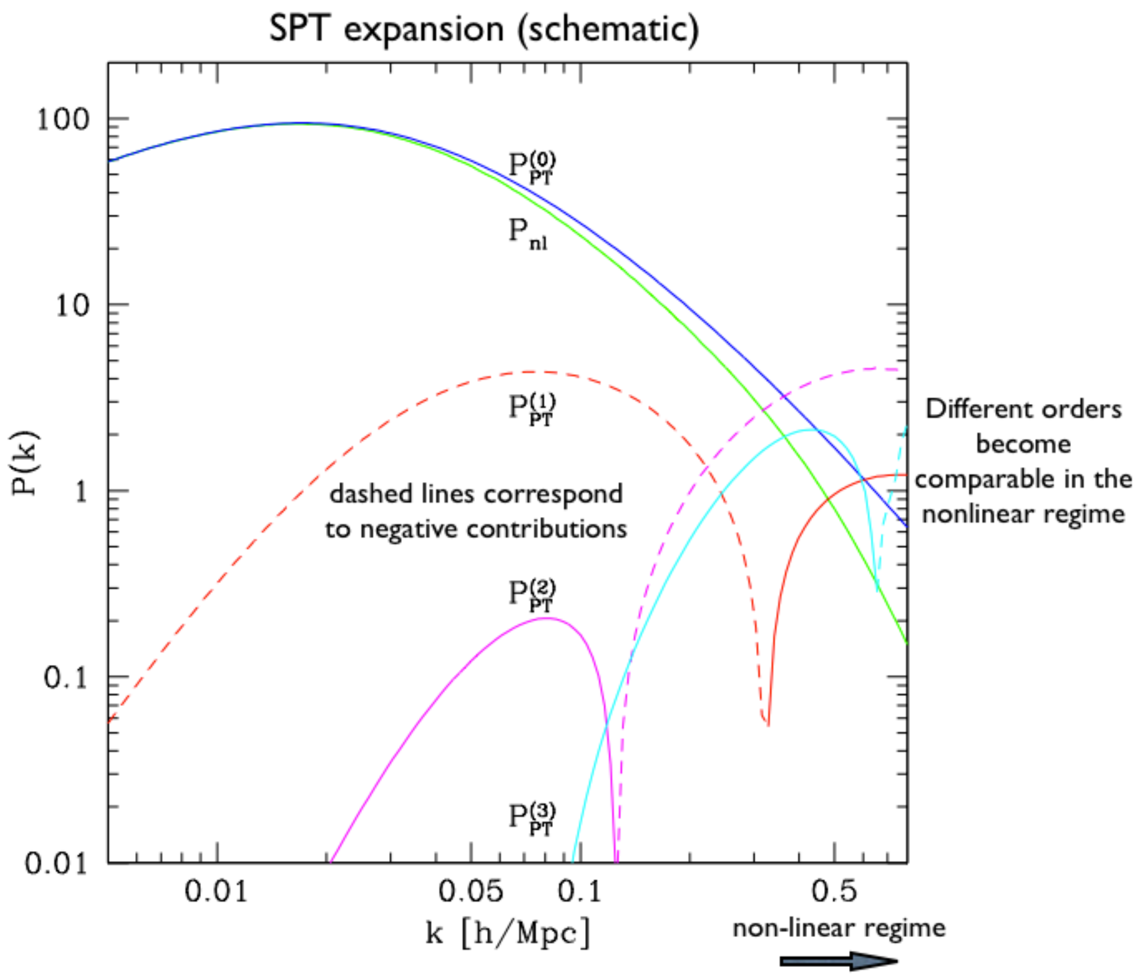

standard PT

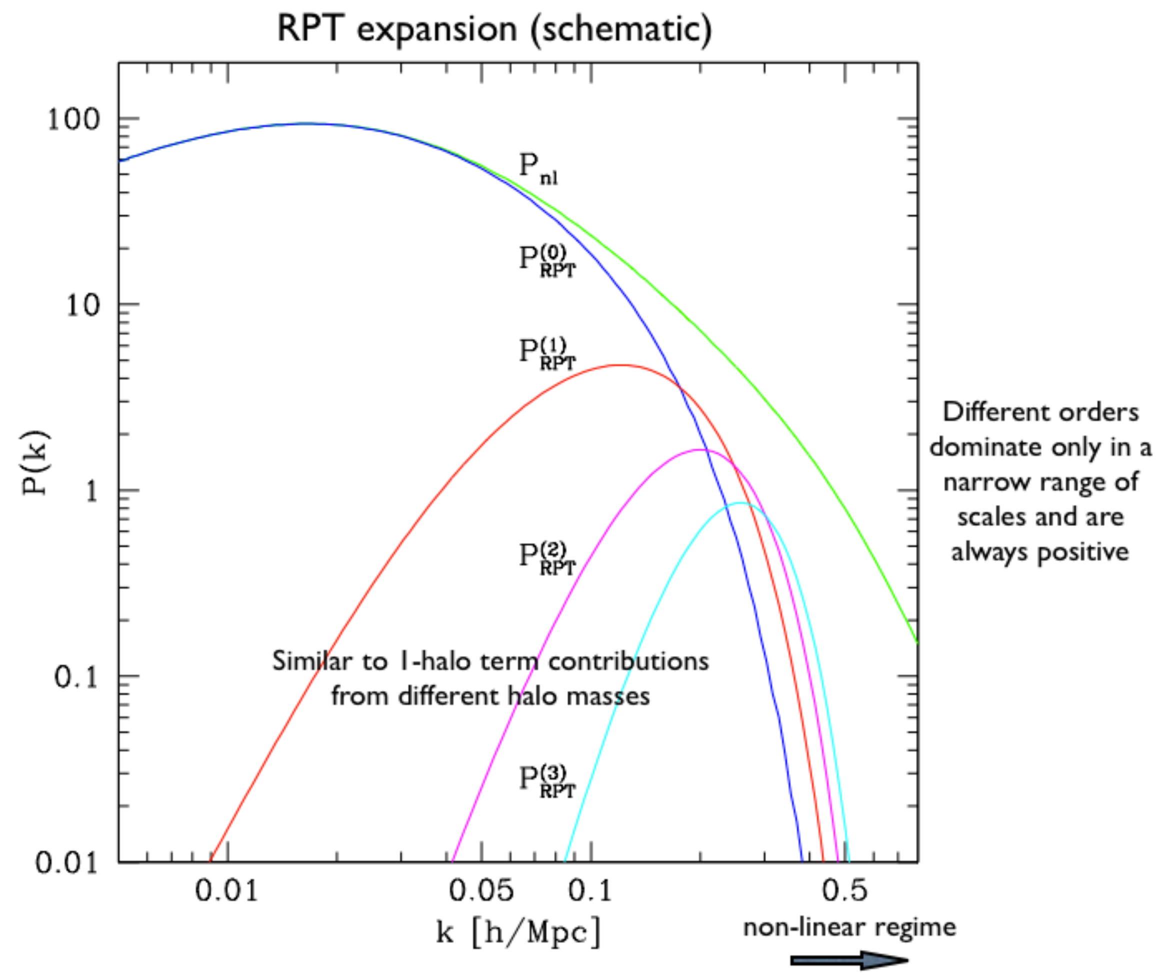

multi-point expansion

Multi-point Propagator Expansion : Density P(k)

We implemented the expansion up to 2 loops (2D and 5D integrations) :

$$
\begin{aligned}
P_{\delta\delta}(k) \;&=\; \left[\Gamma_\delta^{(1)}(k,z)\right]^2 P_0(k) \\
&+\; 2\int d^3q \left[\Gamma_\delta^{(2)}(\mathbf{k}-\mathbf{q},\mathbf{q},z)\right]^2 P_0(|\mathbf{k}-\mathbf{q}|)P_0(q) \\
&+\; 6\int d^3p\, d^3q \left[\Gamma_\delta^{(3)}(\mathbf{k}-\mathbf{p}-\mathbf{q},\mathbf{p},\mathbf{q},z)\right]^2 P_0(|\mathbf{k}-\mathbf{q}|)P_0(p)P_0(q)
\end{aligned}
$$

from PT we know $\Gamma_\delta^{(1)}(k,z) = D(z) - f(k)D^3(z) + \ldots$ **so we take this interpolation between large and small scales :**

$$\checkmark\; \Gamma_\delta^{(1)}(k,z) = G(k,z) = D(z)\exp\left[f(k)D^2(z)\right]$$

And the following ansatze for the MP propagators :
(based on N-body results)

$$
\left\{
\begin{aligned}
&\checkmark\; \Gamma_\delta^{(2)} = G(k,z) \times F_2 \\
&\checkmark\; \Gamma_\delta^{(3)} = G(k,z) \times F_3
\end{aligned}
\right.
$$

with F_2 and F_3 the standard PT kernels and

$$f(k) \;=\; \int \frac{1}{504k^3q^5}\left[6k^7q - 79k^5q^3 + 50q^5k^3 - 21kq^7 + \frac{3}{4}(k^2-q^2)^3(2k^2+7q^2)\ln\frac{|k-q|^2}{|k+q|^2}\right] P_0(q)\, d^3q,$$

Suite of Cosmological Simulations

Run	Ω_m	Ω_b	h	σ_8	n_s	$L_{box}(h^{-1}\,\mathrm{Mpc})$	N_{runs}	k_{nl}(z=0,0.5,1)
FID	0.27	0.04	0.7	0.9	1	1280	50	0.15 - 0.2 - 0.25
tilt					0.9	1250	4	
WMAP3	0.2383	0.0418	0.73	0.74	0.95	1250	4	
Low-Ω_m	0.20					1250	4	
Mid-σ_8				0.8		1250	4	
Low-σ_8				0.7		1250	4	
Las Damas	0.25	0.044	0.7	0.8	1	2400	4	

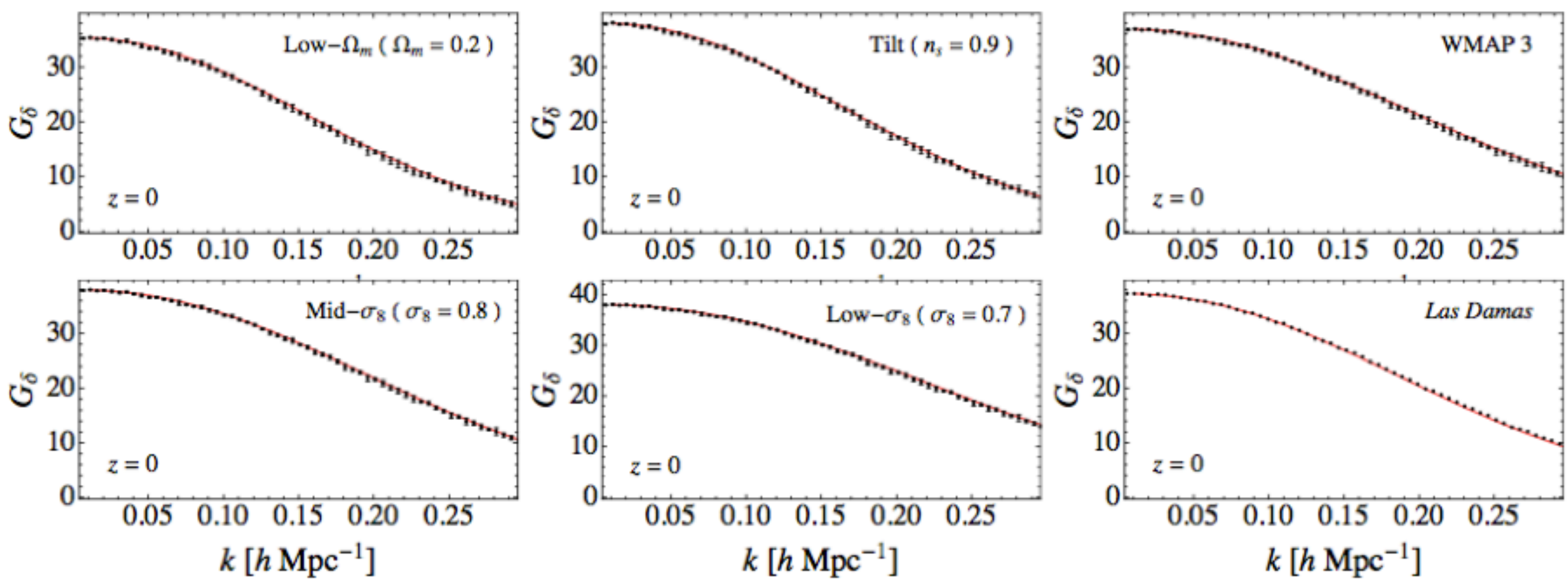

Power Spectrum (MPTbreeze)

performance for different cosmological models at z=0

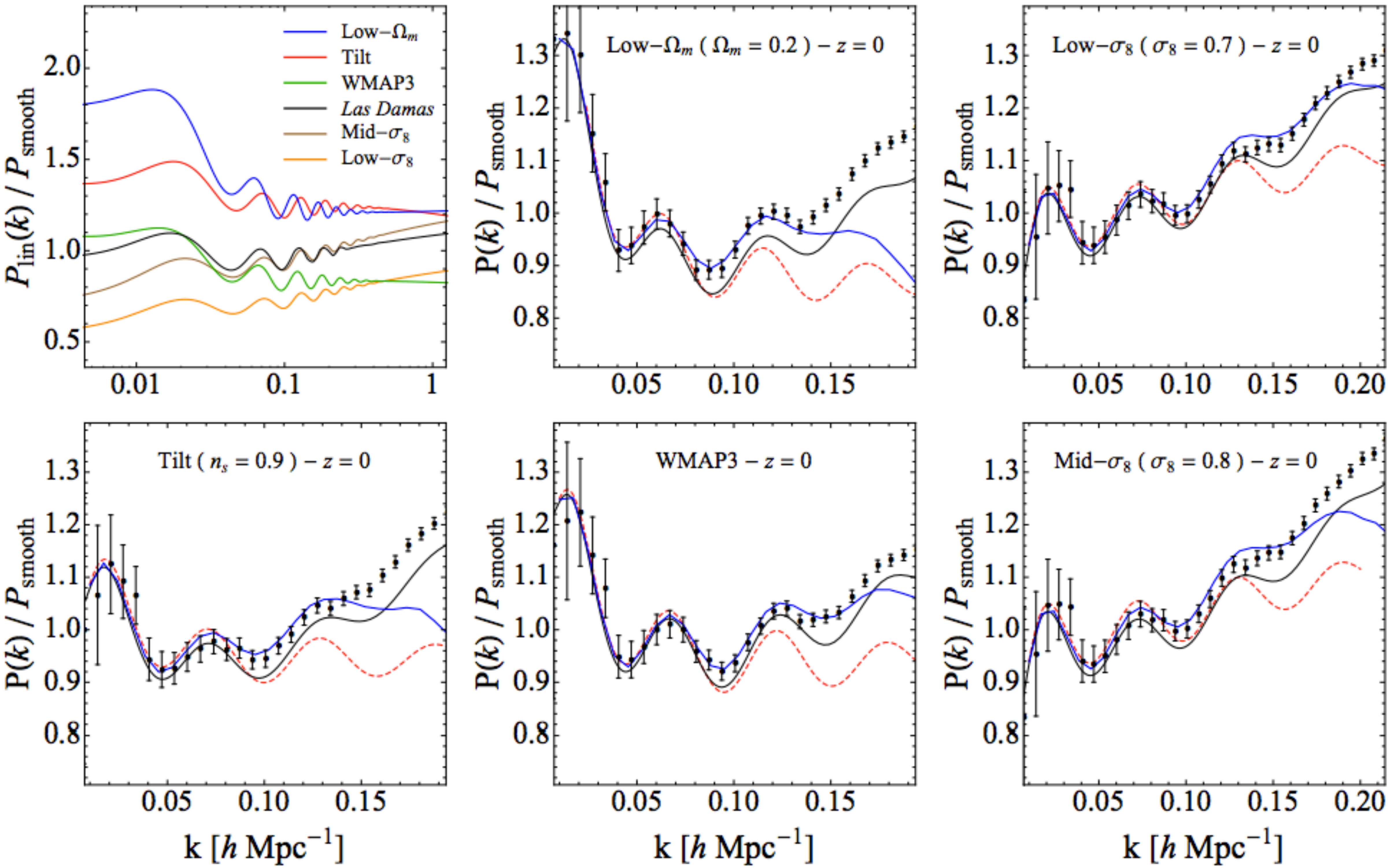

only few seconds of evaluation time !!

Power Spectrum (MPTbreeze)

performance for different cosmological models at higher redshift

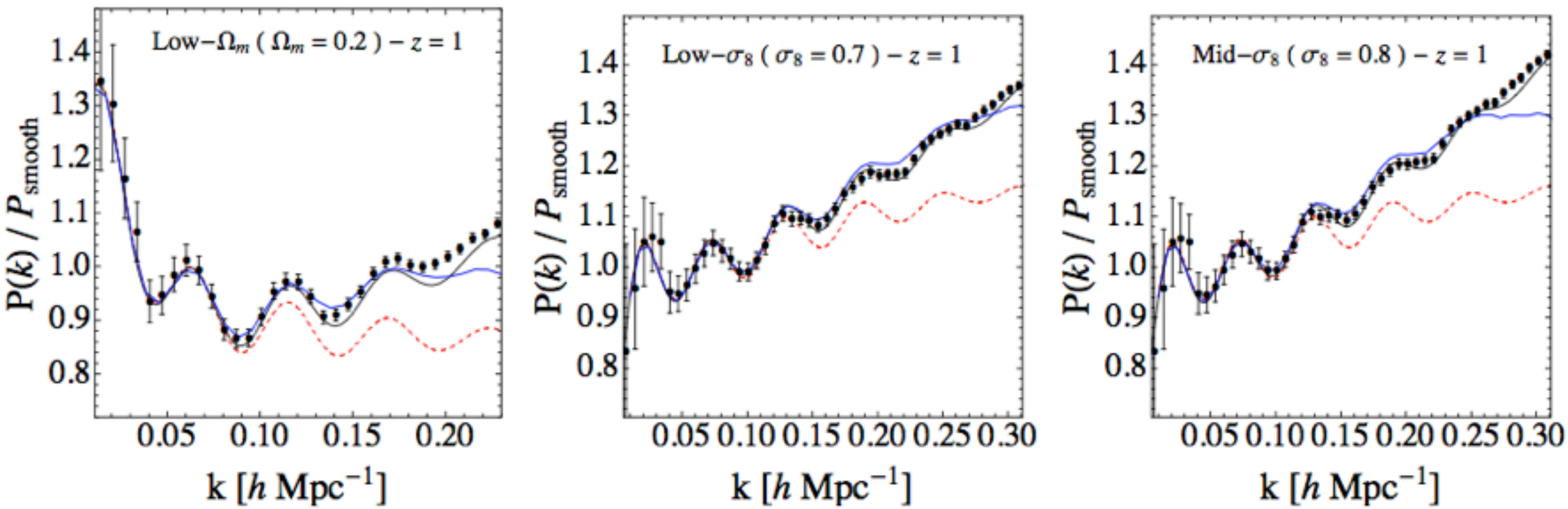

MPTbreeze
code is publicly available at http://maia.ice.cat/crocce/mptbreeze

see Crocce, Scoccimarro and Bernardeau (2012)

Also orthogonality plus the fact that propagators decay as Gaussians, means in real space each loop is also (as good as possible) localized and contributions are ordered in r.

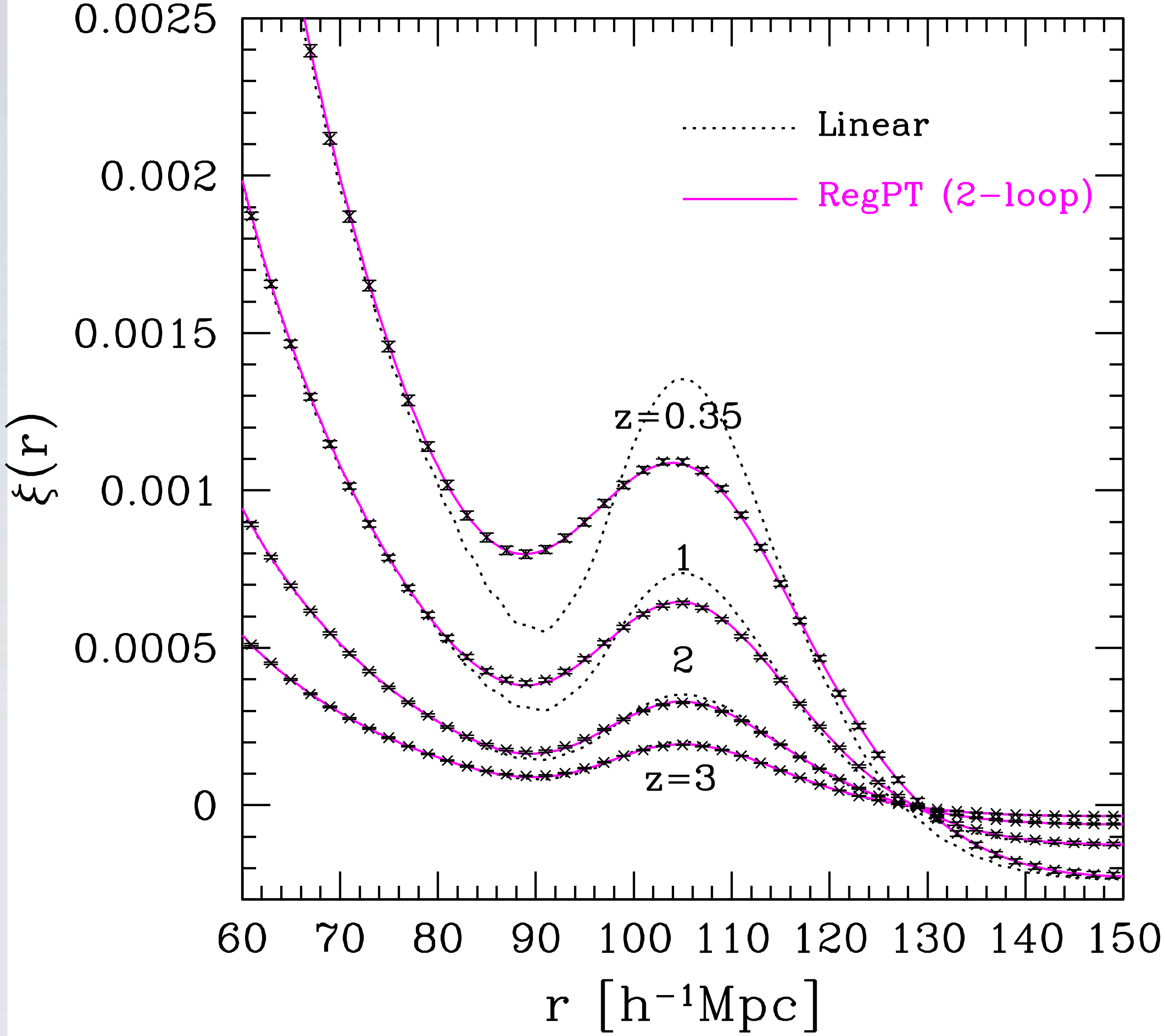

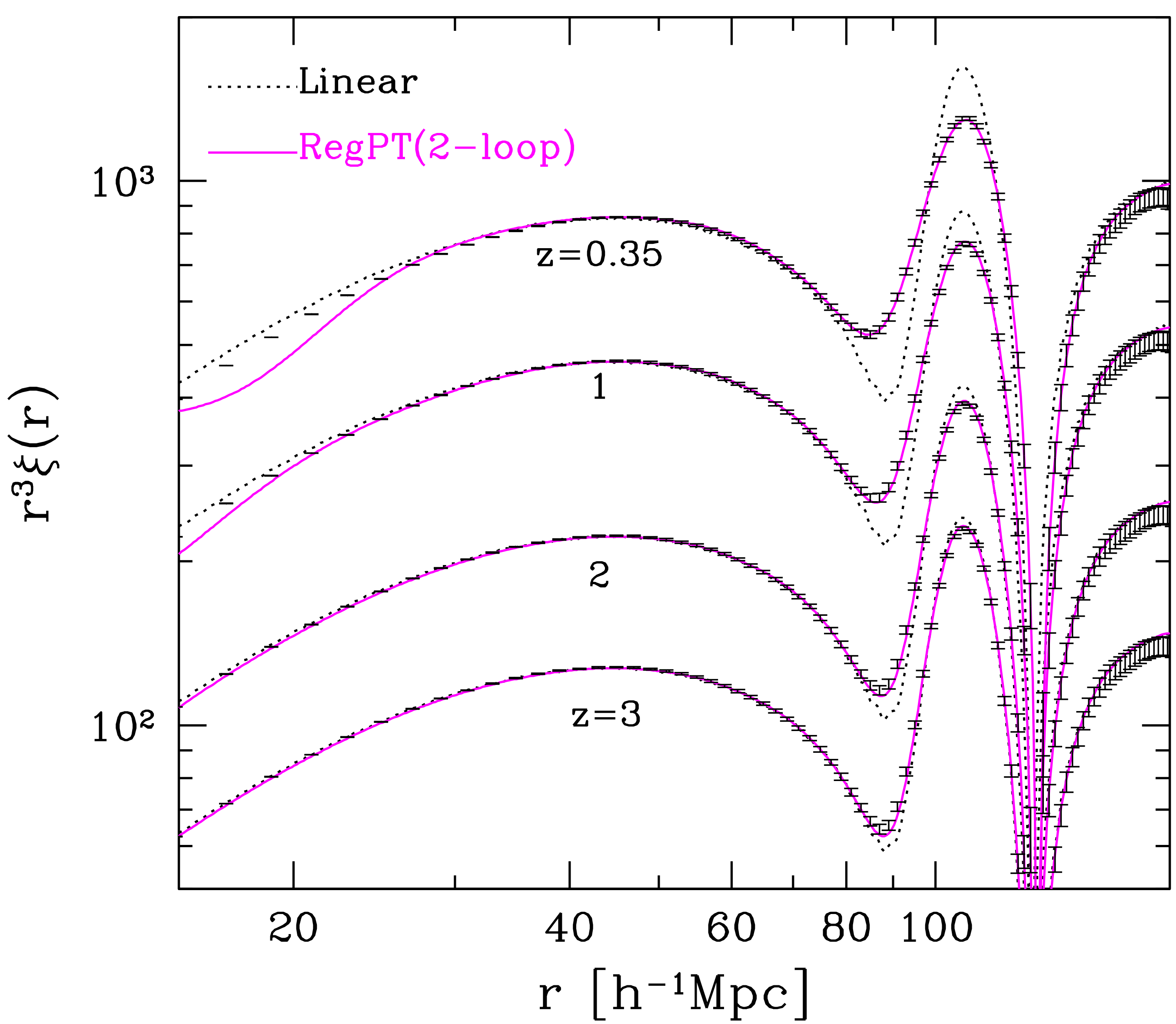

RegPT code : Taruya, Bernardeau, Nishimichi, Codis (2012)

Improvement

it is possible to use the symmetries of the equations of motion (concretely galilean invariance) to understand how the mode-coupling term re-sums

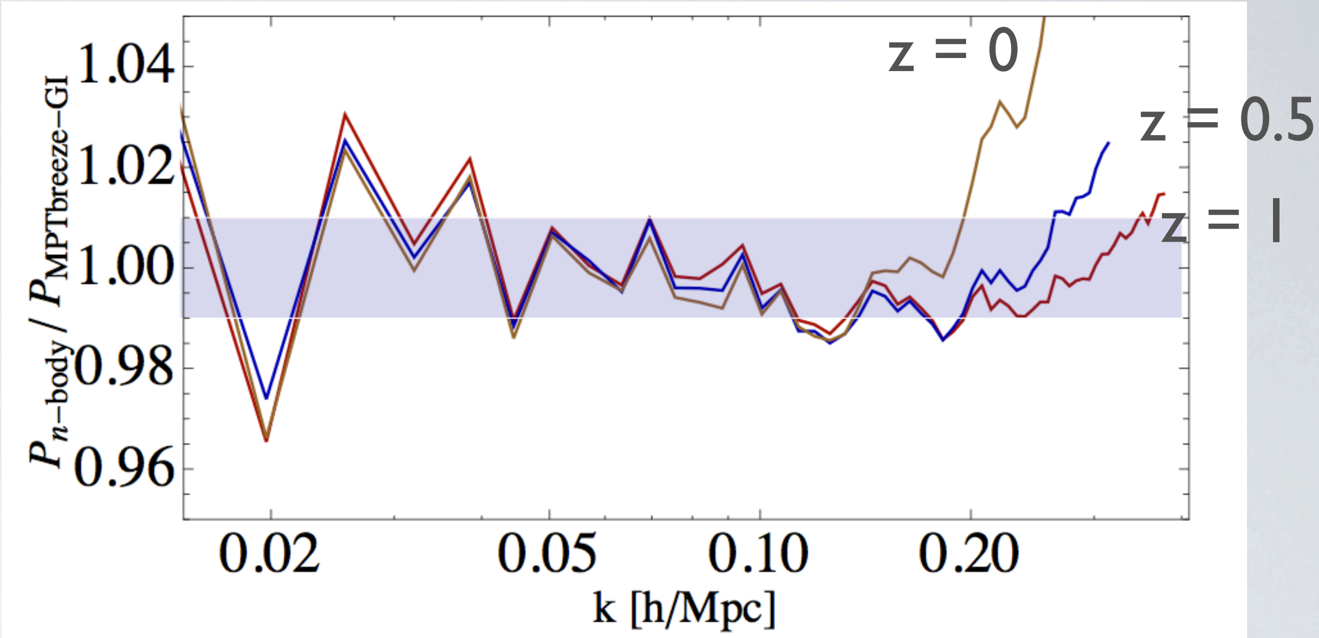

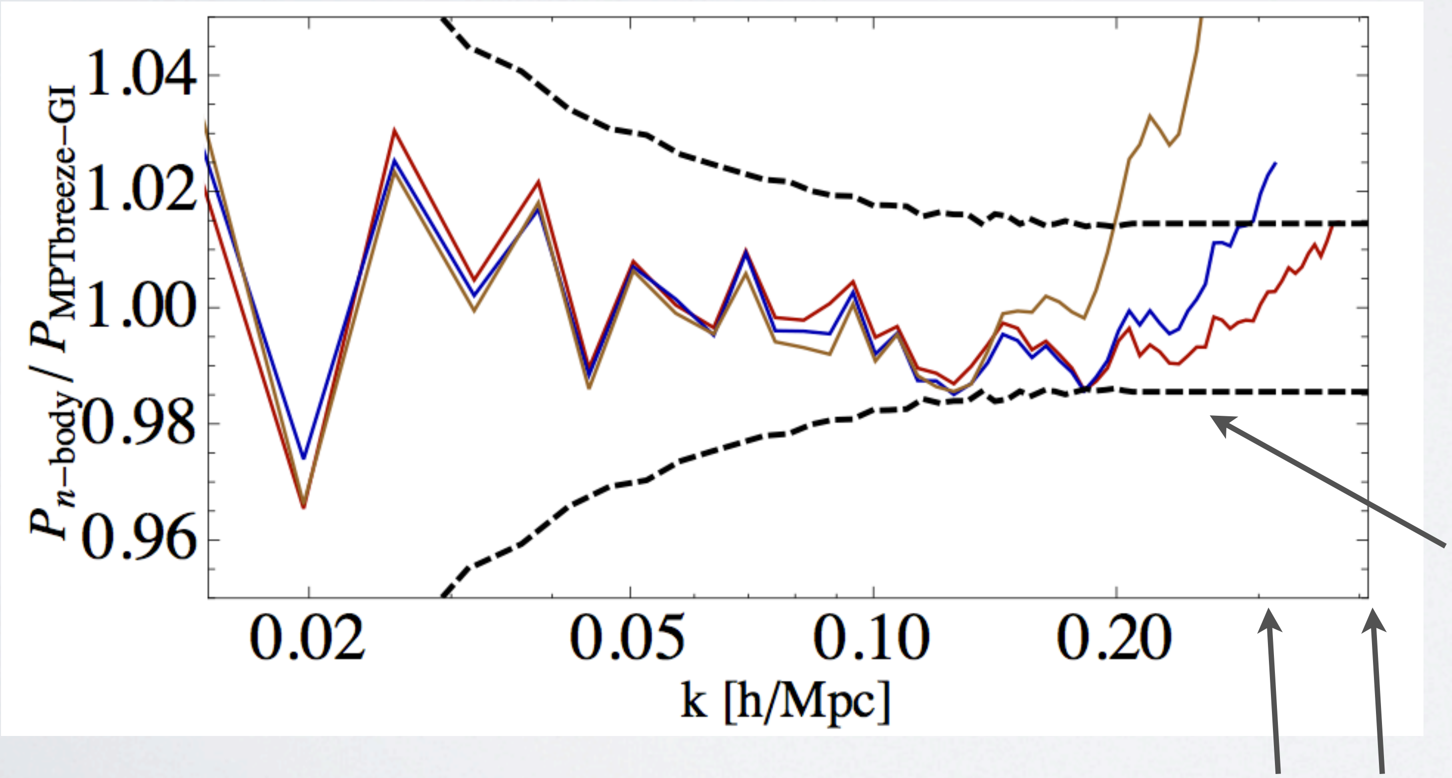

Works up to k ~ 0.3 at z=0.5 and k ~ 0.4 at z=1 (using one-loop RPT).

Running time is < 10 seconds.

Better than BOSS precision

Published soon ... ()

Let us now move more into the simulation side of things ..

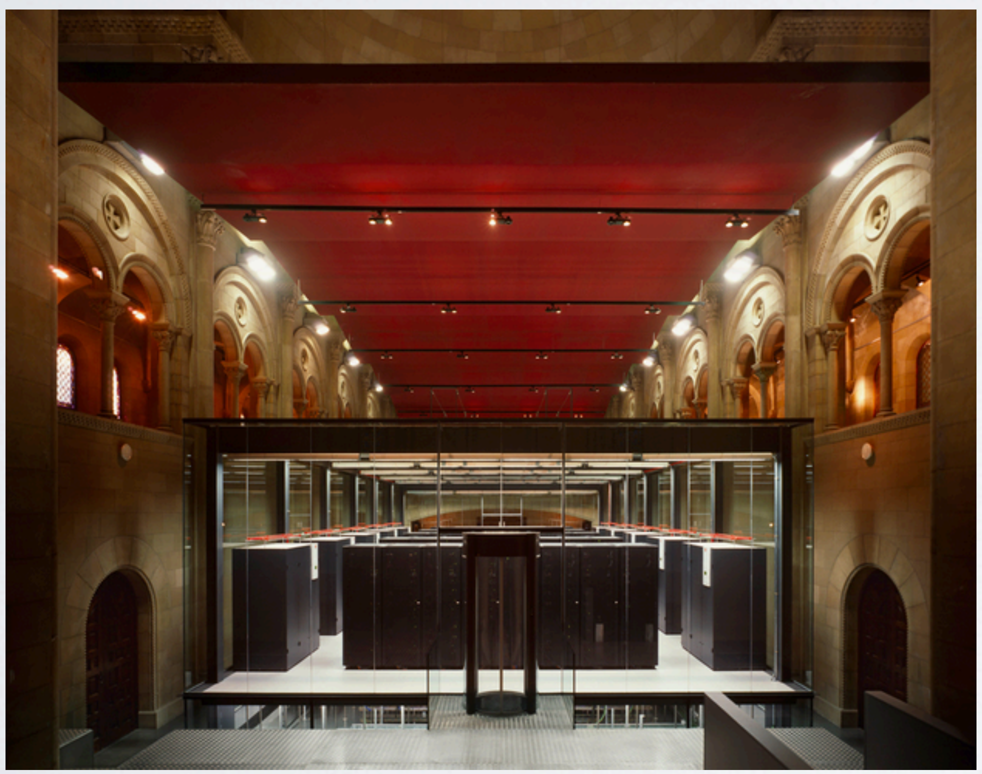

The MICE simulations and the grand challenge run

Run	$N_{\rm part}$	$L_{\rm box}/h^{-1}$ Mpc	*PMGrid*	$m_p/(10^{10}\,h^{-1}\,{\rm M}_\odot)$	$l_{\rm soft}/h^{-1}$ Kpc	$z_{\rm i}$	*Max.TimeStep*
MICE-GC	4096^3	3072	4096	2.93	50	100	0.02
MICE-IR	2048^3	3072	2048	23.42	50	50	0.01
MICE-SHV	2048^3	7680	2048	366	50	150	0.03

- MICE collaboration :: GADGET N-body simulations with $10^9 \sim 10^{12}$ DM particles within 1-500 h^{-3} Gpc^3 dynamical range of 5-6 orders of magnitude

- Marenostrum Supercomputer: 10.000 processors, 20 TB RAM , 100 Teraflops

- More than 50 Terabytes of simulated data stored at Port d'Informació Cientifica (LHC data storage center @ Barcelona)

Series of papers for MICE-GC = Fosalba et a. 2014, Crocce et al. 2014, Carretero et al 2014

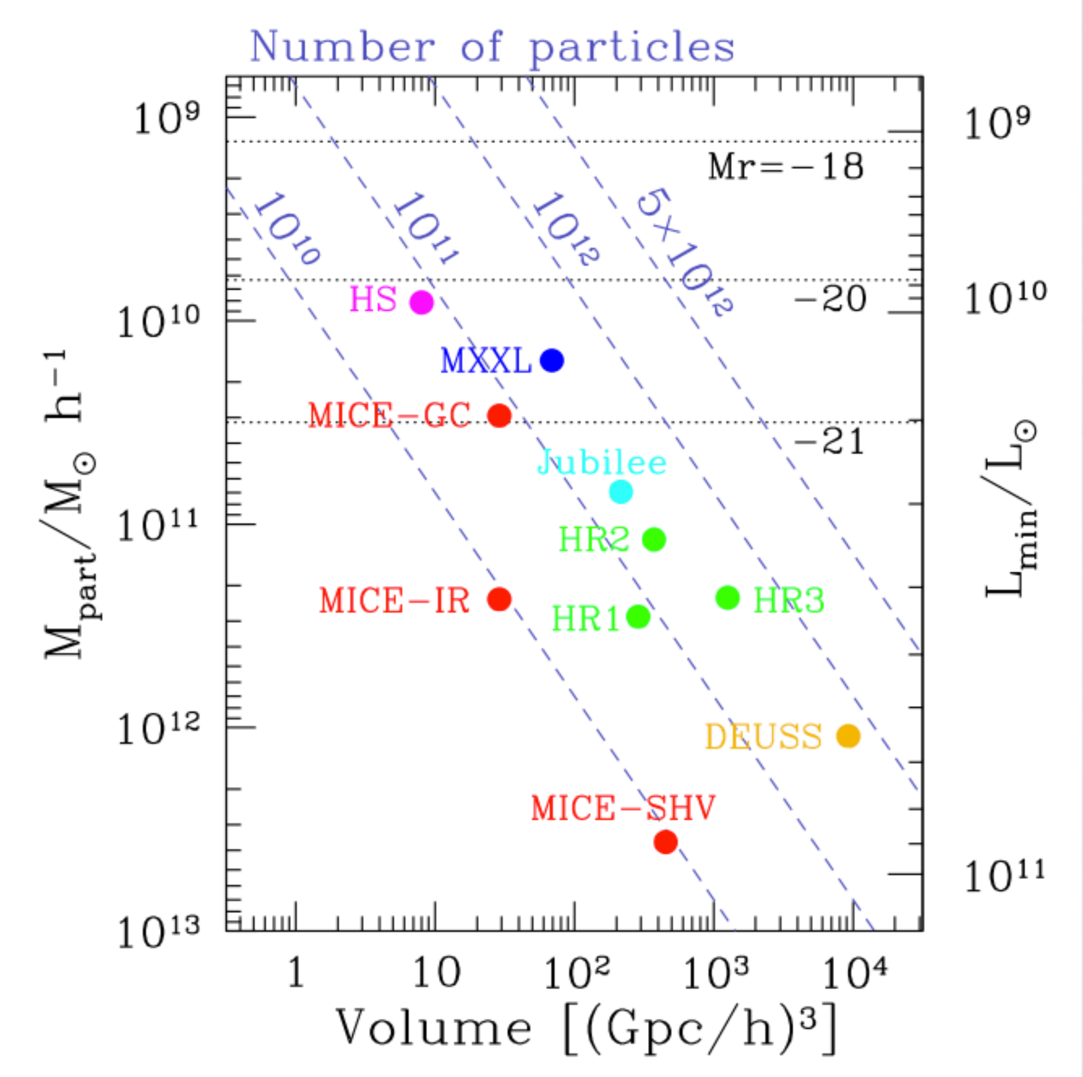

The MICE grand challenge simulation

- The MICE-Grand Challenge N-body simulation 70 billion particles with a DES-like volume (particle mass 3×10^{10} Msun/h)

Run	$N_{\rm part}$	$L_{\rm box}/\,h^{-1}\,{\rm Mpc}$	$PMGrid$	$m_p/(10^{10}\,h^{-1}\,{\rm M}_\odot)$	$l_{\rm soft}/\,h^{-1}\,{\rm Kpc}$	$z_{\rm i}$	$Max.TimeStep$
MICE-GC	4096^3	3072	4096	2.93	50	100	0.02

- Full sky light-cone with minimal repetition up to z=1.4 + lensing maps

- Stored co-moving outputs outputs at several redshifts (0 0.5 1 etc). 1TB each.

- End-to-End : dark matter - halos - galaxies (abundance / clustering / lensing) - public data

- Lets start by looking at the dark matter clustering in MICE-GC and compare it with previous runs and state-of-the-art modeling and fits.

The MICE grand challenge simulation : dark matter at large scales

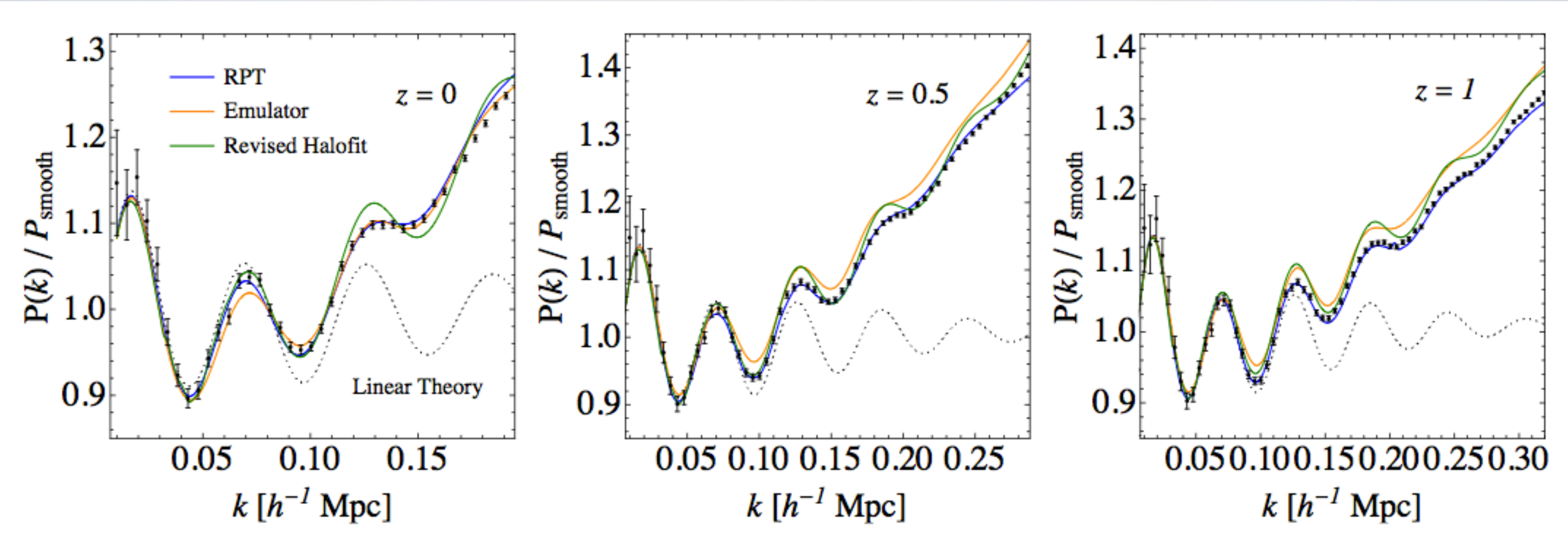

- State-of-the-Art numerical fits include Coyote and Halofit from Takahasi et al 2012.

- Coyote works very well at z=0 and slightly over-estimate the overall amplitude at z = 0.5 and 1 by ~ 2% (but BAO wiggles are well traced, not the case for Halofit +)

- Renormalized PT (Crocce and Scoccimarro 08) works well up to k ~ 0.2 - 0.3 h/Mpc (@ to z = 0 - 1)

Moving onto configuration space

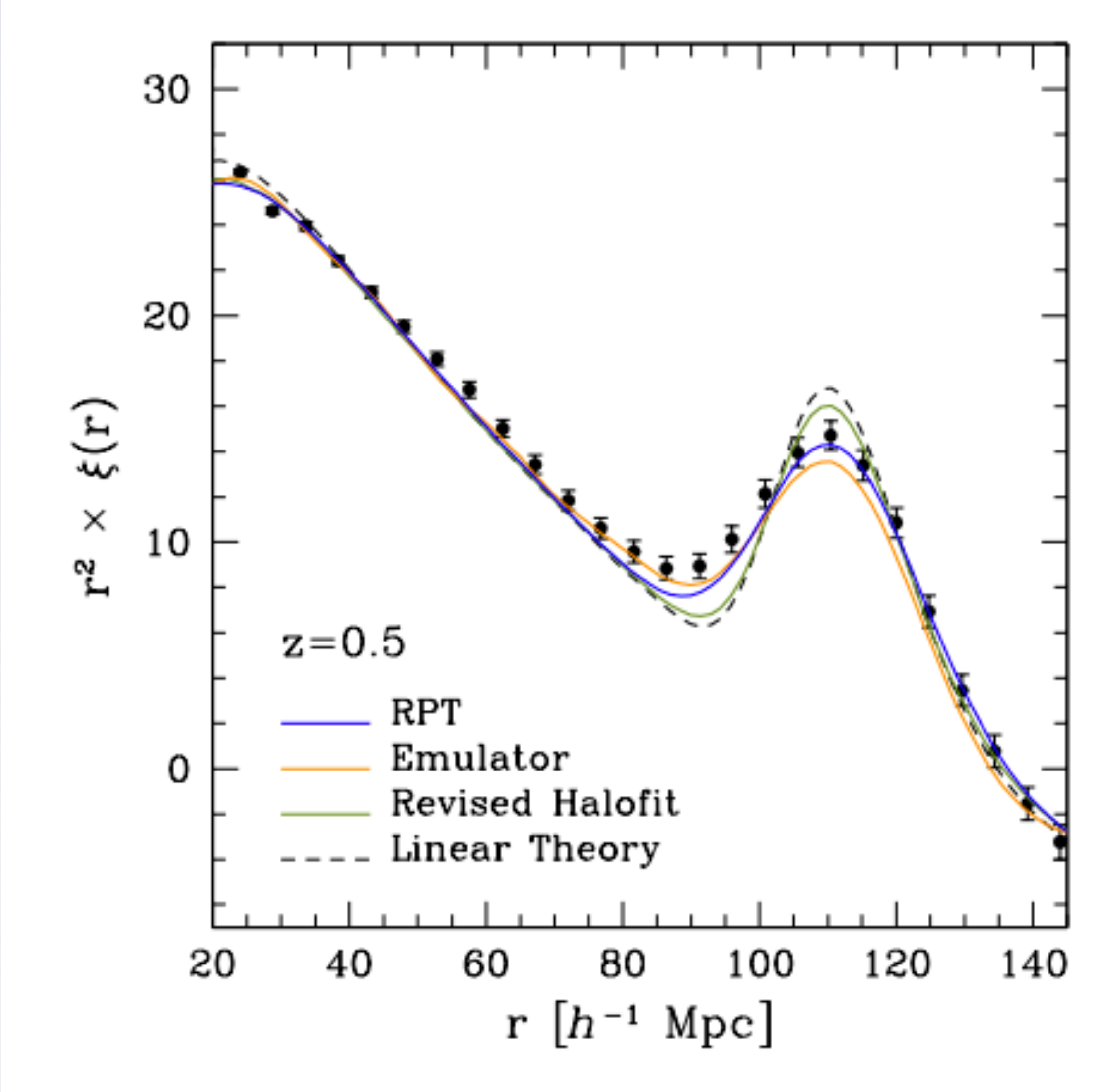

- But recall that data points in correlation function are quite correlated

The MICE grand challenge simulation : dark matter clustering to small scales

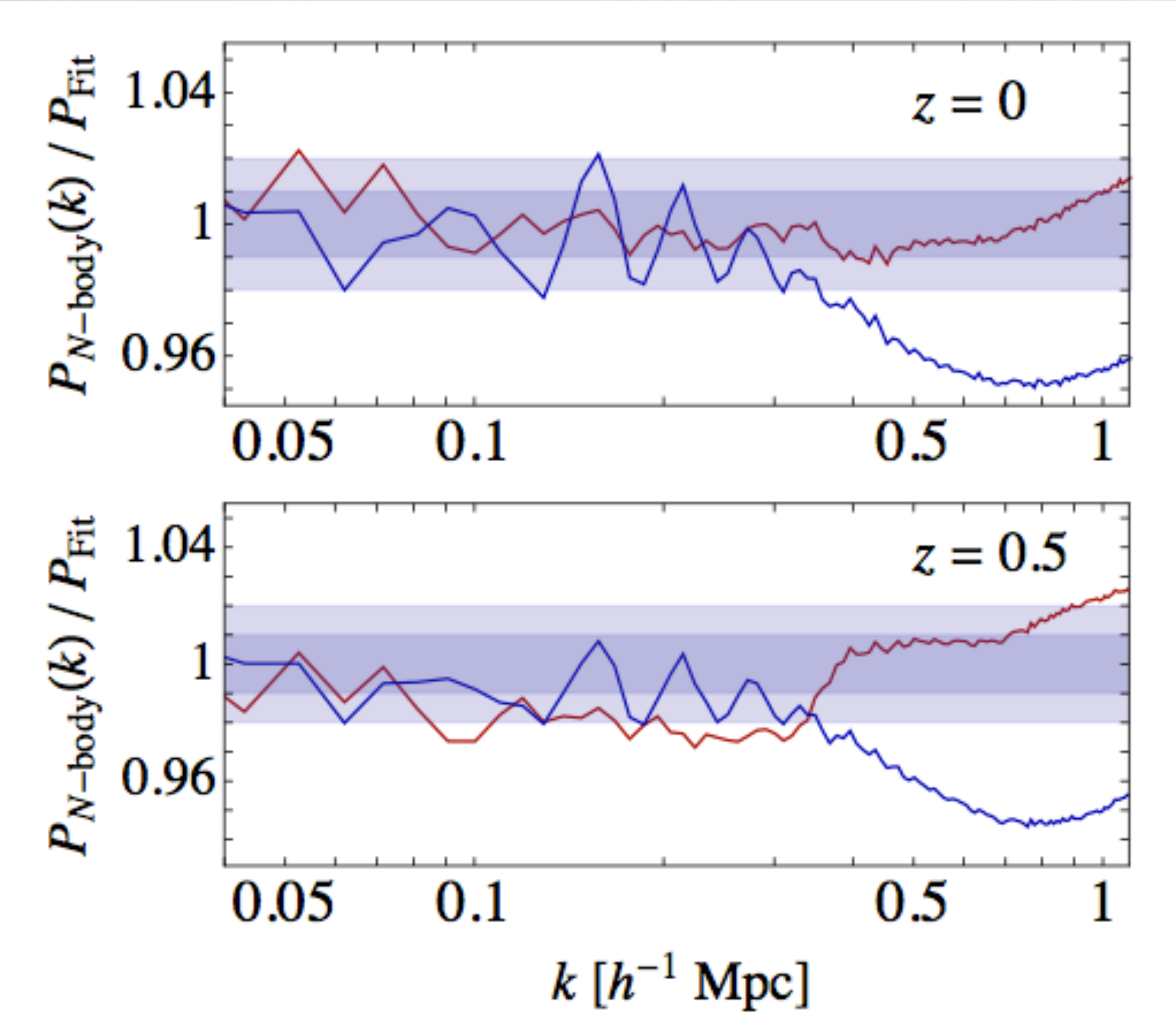

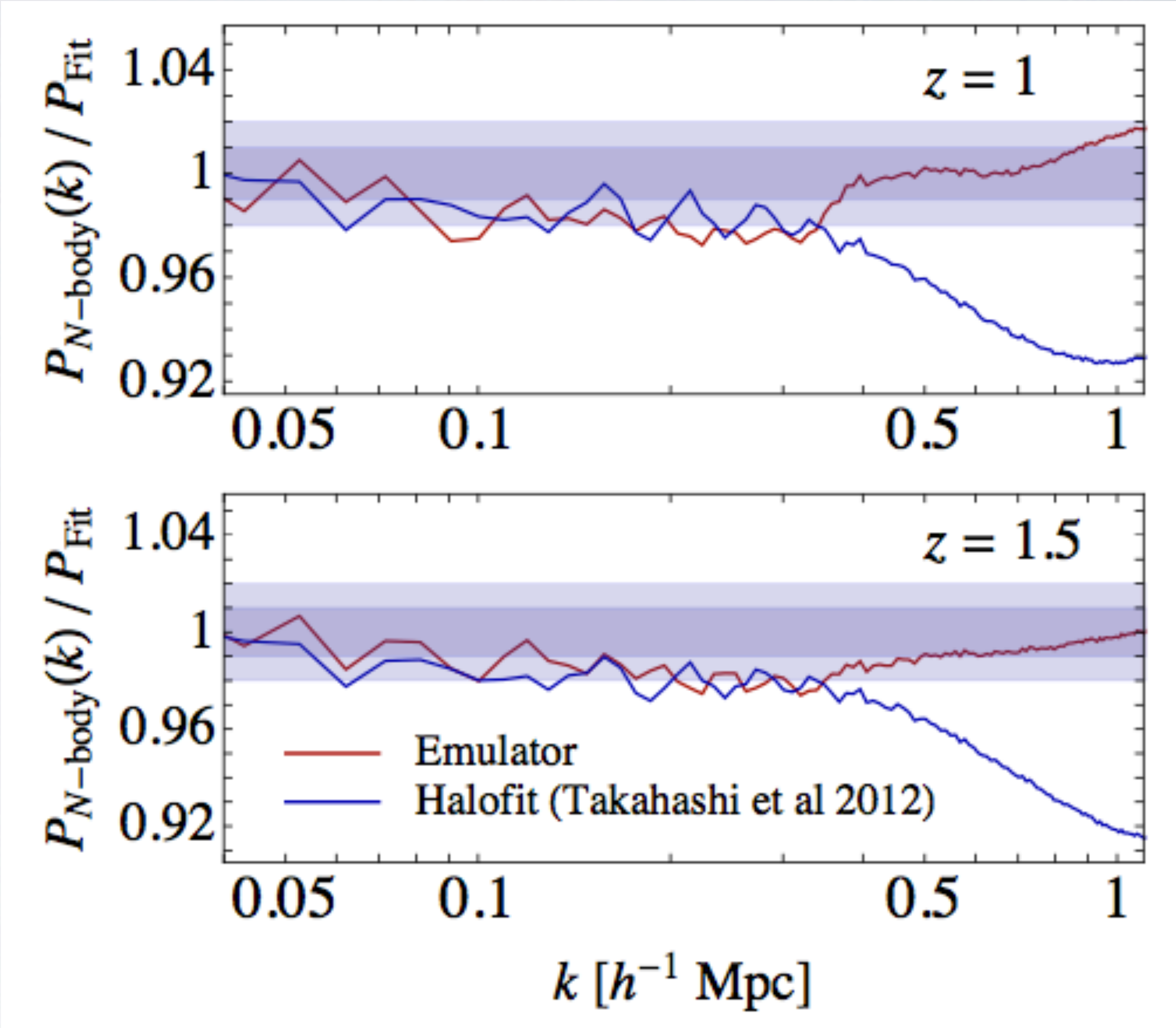

- Coyote Emulator is within 2-3 % or so all the way to k ~ 1 h/Mpc (note some jump at k ~ 0.5 h/Mpc)

- Halofit + can over-estimate by 5 - 8 % particularly at higher z.

The MICE grand challenge simulation : dark matter clustering in z-bins

Modeling the dark-matter : arc-min scale clustering and impact of redshift space distortions

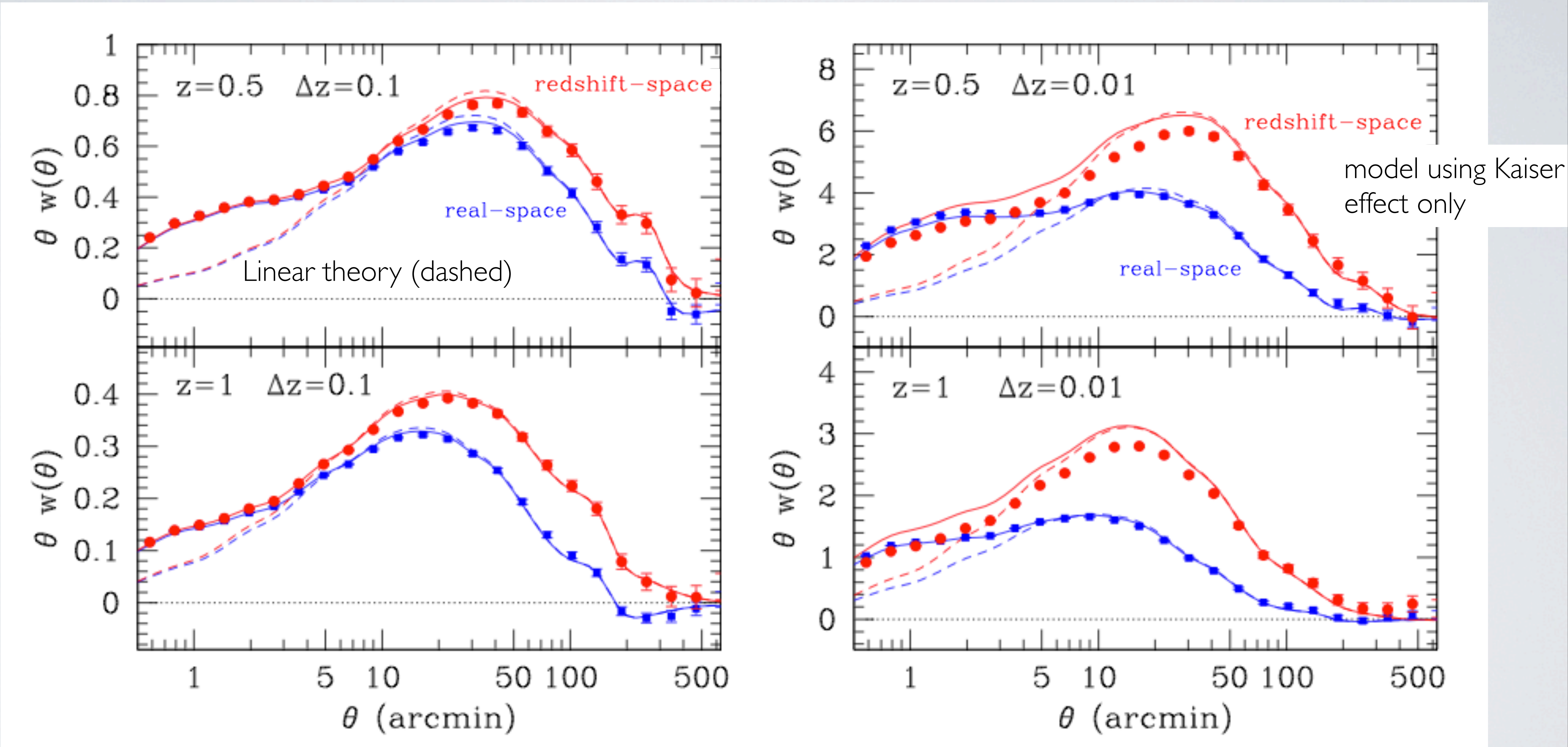

Typical bins used by broad-band imaging surveys as DES

Narrower bins than can be implemented in say BOSS

The MICE grand challenge simulation : mass resolution effects

Power Spectrum

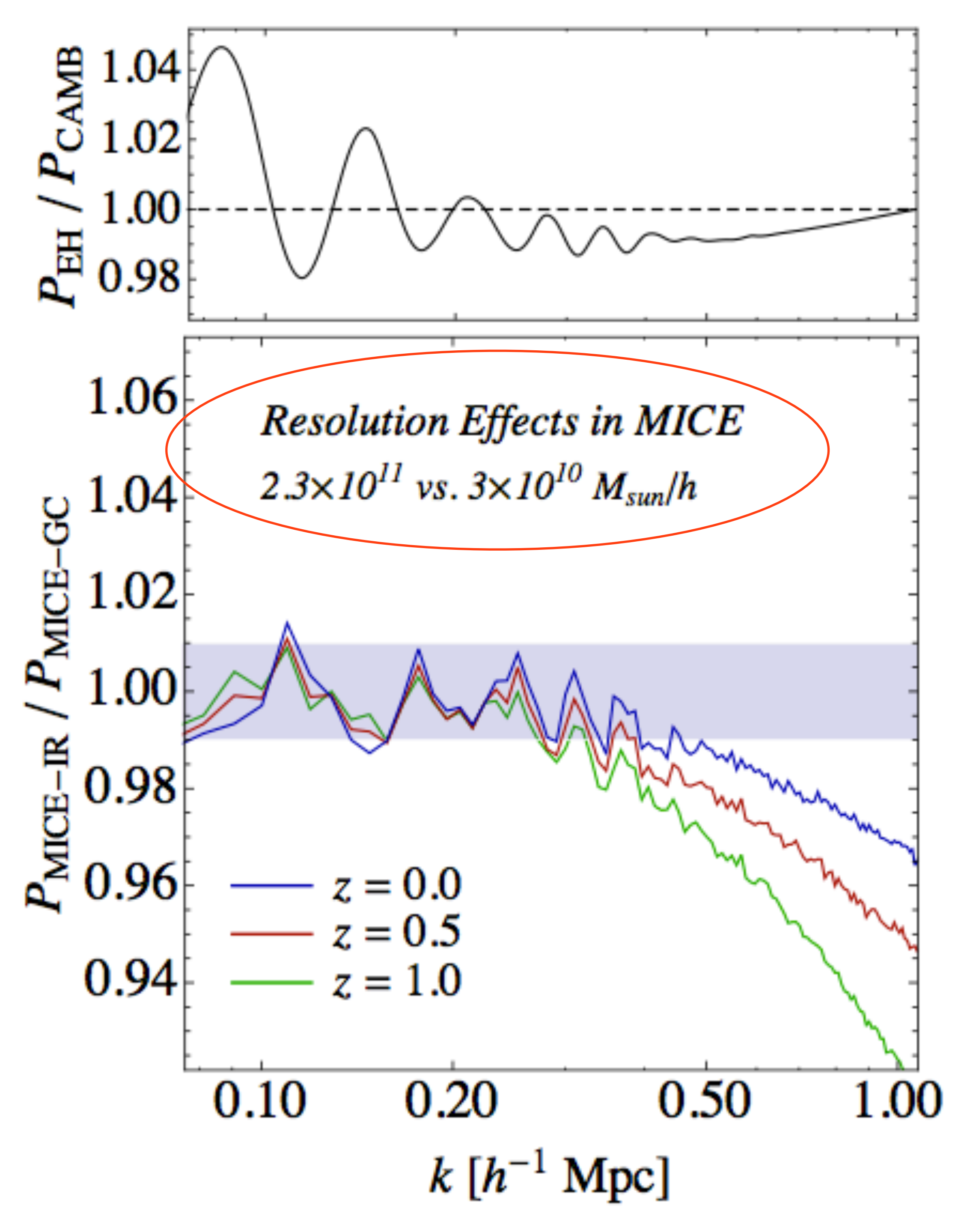

Reduced 3-point function

$$Q_3 = \frac{\zeta(r_{12}, r_{23}, r_{13})}{\zeta_H(r_{12}, r_{23}, r_{13})}$$

$$\zeta_H \equiv \xi(r_{12})\xi(r_{23}) + \xi(r_{12})\xi(r_{13}) + \xi(r_{23})\xi(r_{13})$$

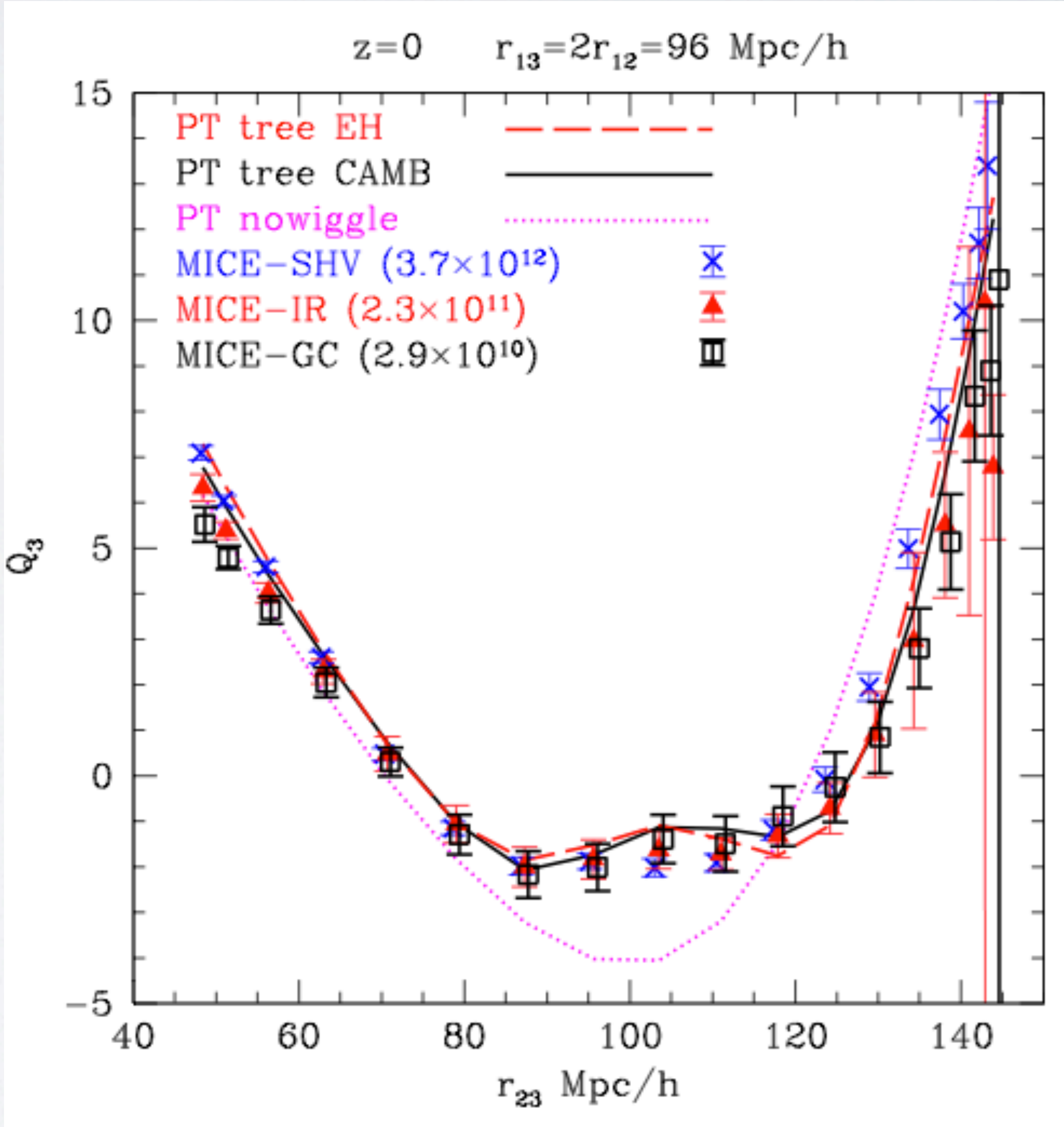

- higher resolution yields more power in general, large scales seem less affected

The MICE grand challenge simulation : mass resolution effects

Power Spectrum

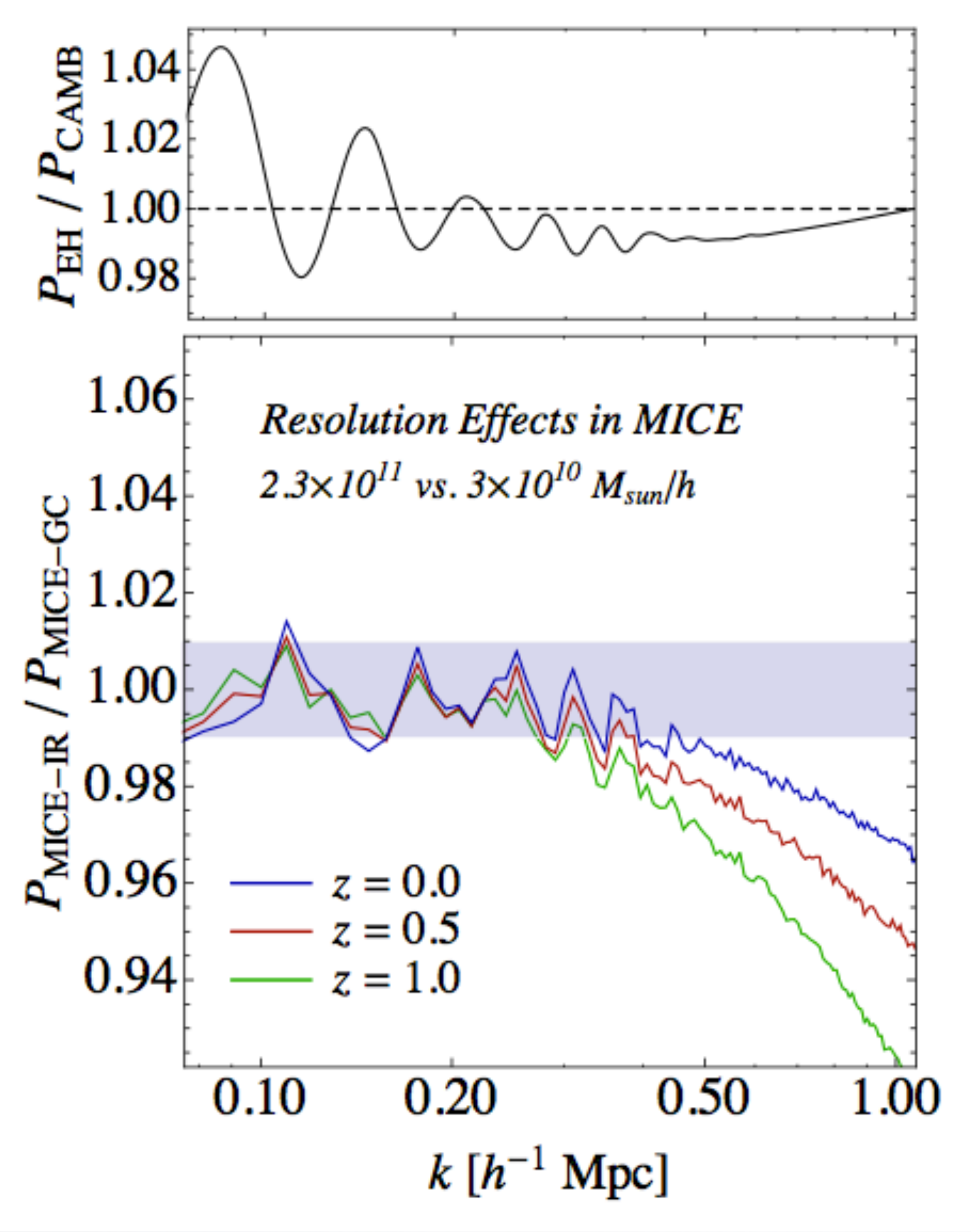

Reduced 3-point function

$$
\begin{aligned}
Q_3 &= \frac{\zeta(r_{12}, r_{23}, r_{13})}{\zeta_H(r_{12}, r_{23}, r_{13})} \\
\zeta_H &\equiv \xi(r_{12})\xi(r_{23}) + \xi(r_{12})\xi(r_{13}) + \xi(r_{23})\xi(r_{13})
\end{aligned}
$$

smaller scales

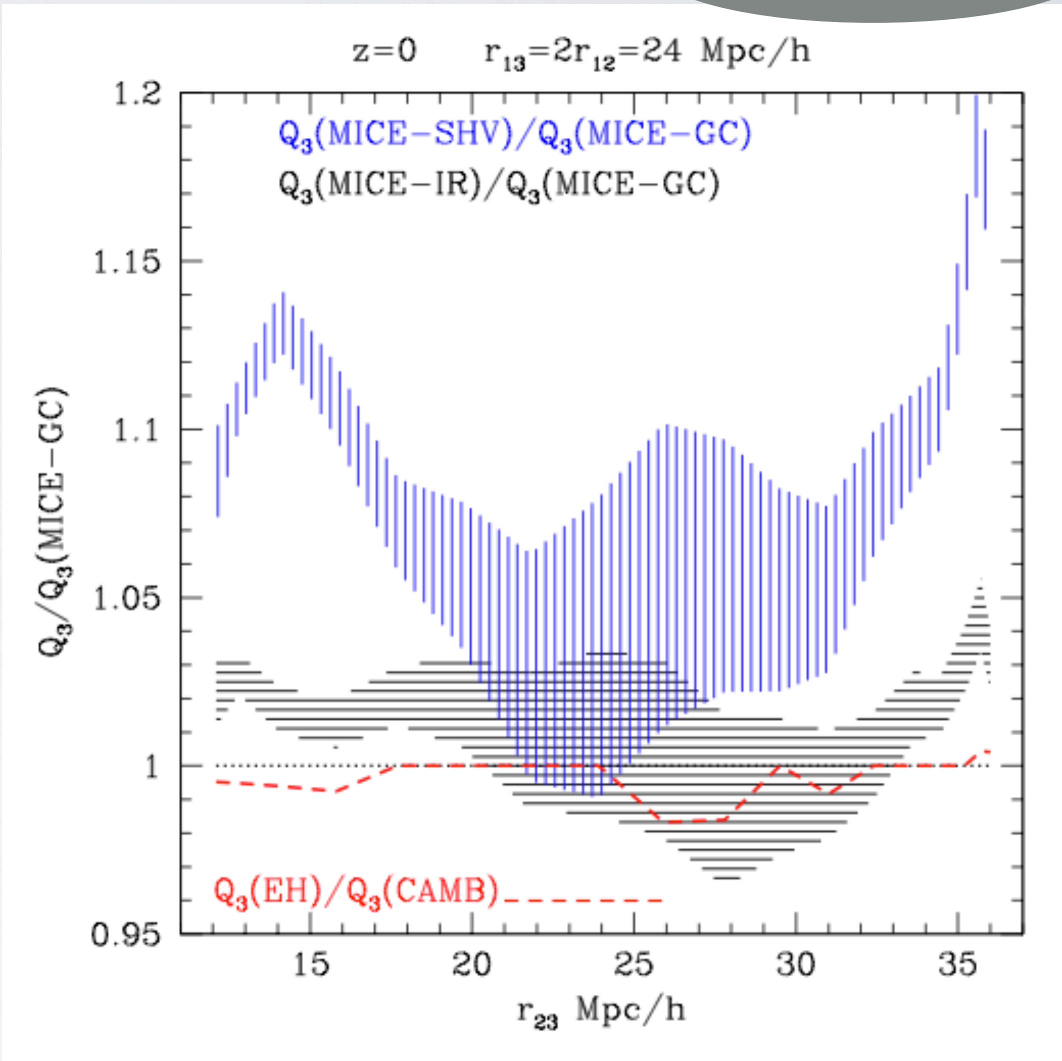

- better mass resolution makes the clustering more isotropic (less Q3 amplitude)

The MICE halo catalog

Mass resolution effects in halo bias from 2-pt clustering

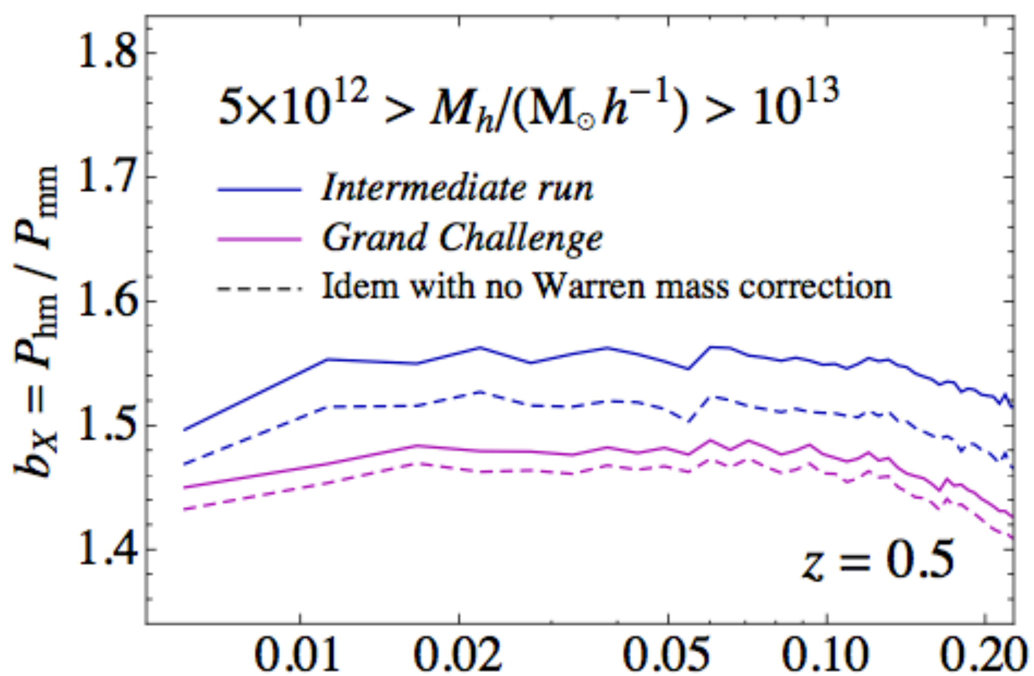

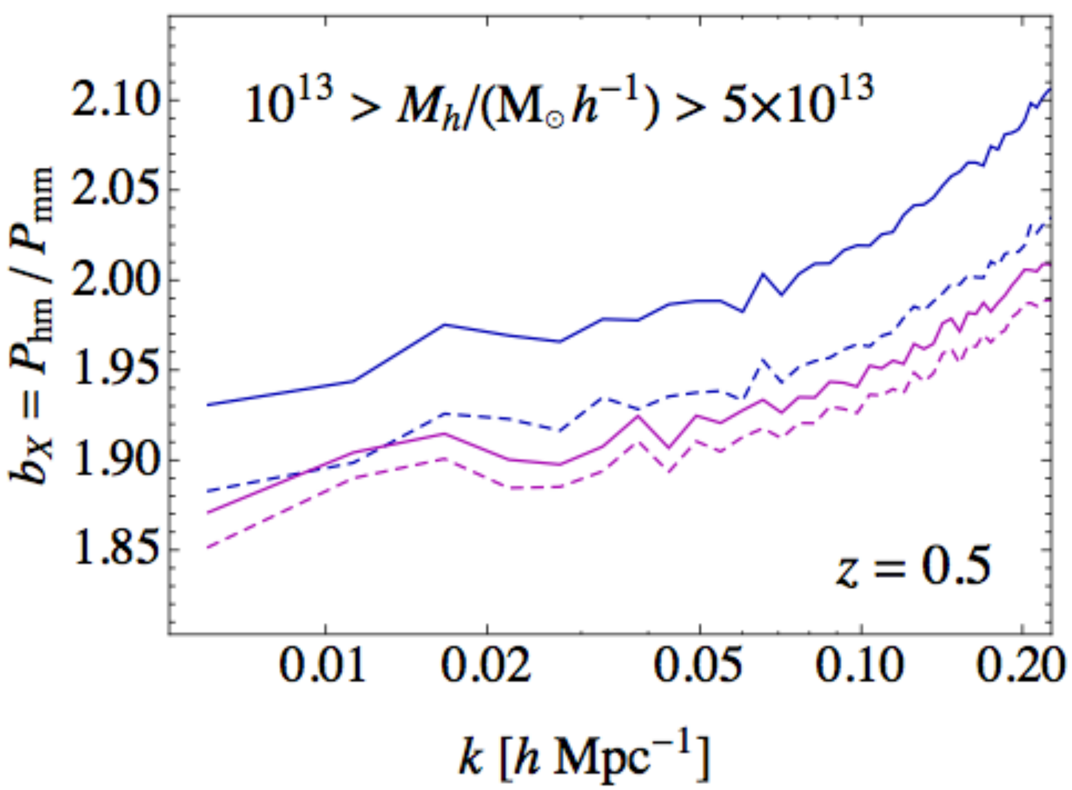

Low Mass (20-50 particles)
Mid Mass (50-200)
High Mass (>200) and 10 times ore in MICE-GC

For poorly resolved halos there is a 4% effect for standardly defined FoF mass and up to 6% if Warren correction is included. The effect goes away for 200 or more particles

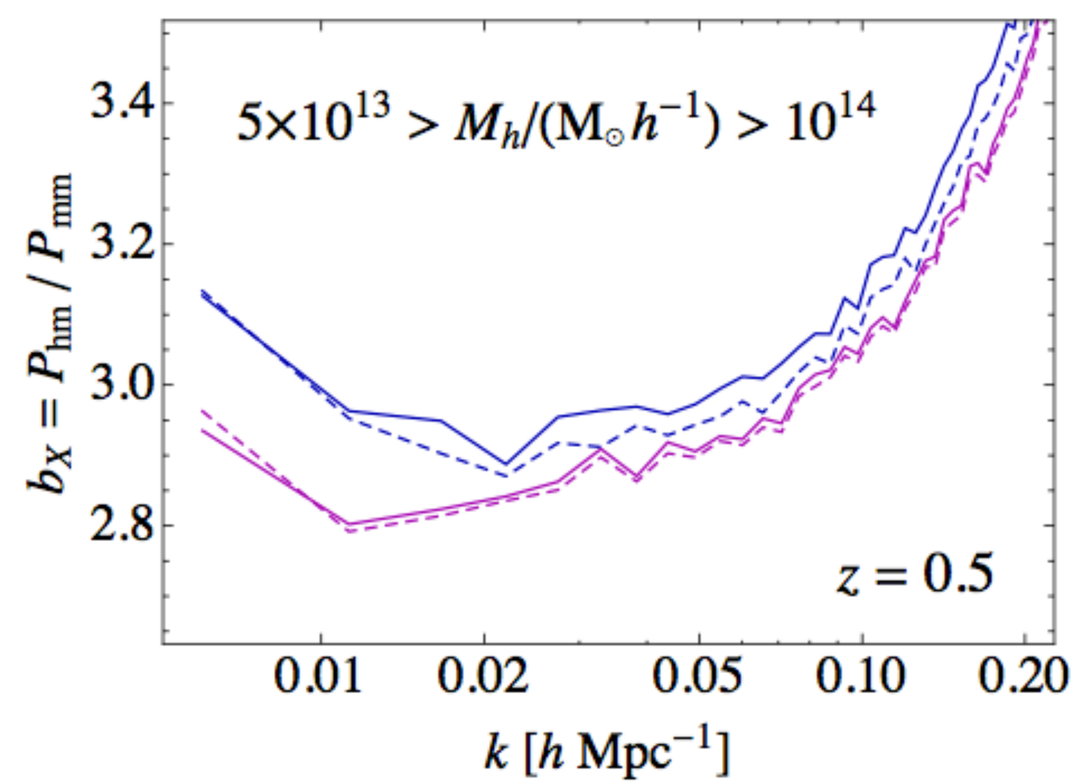

The MICE halo catalog

Mass resolution effects in halo bias from 3-pt

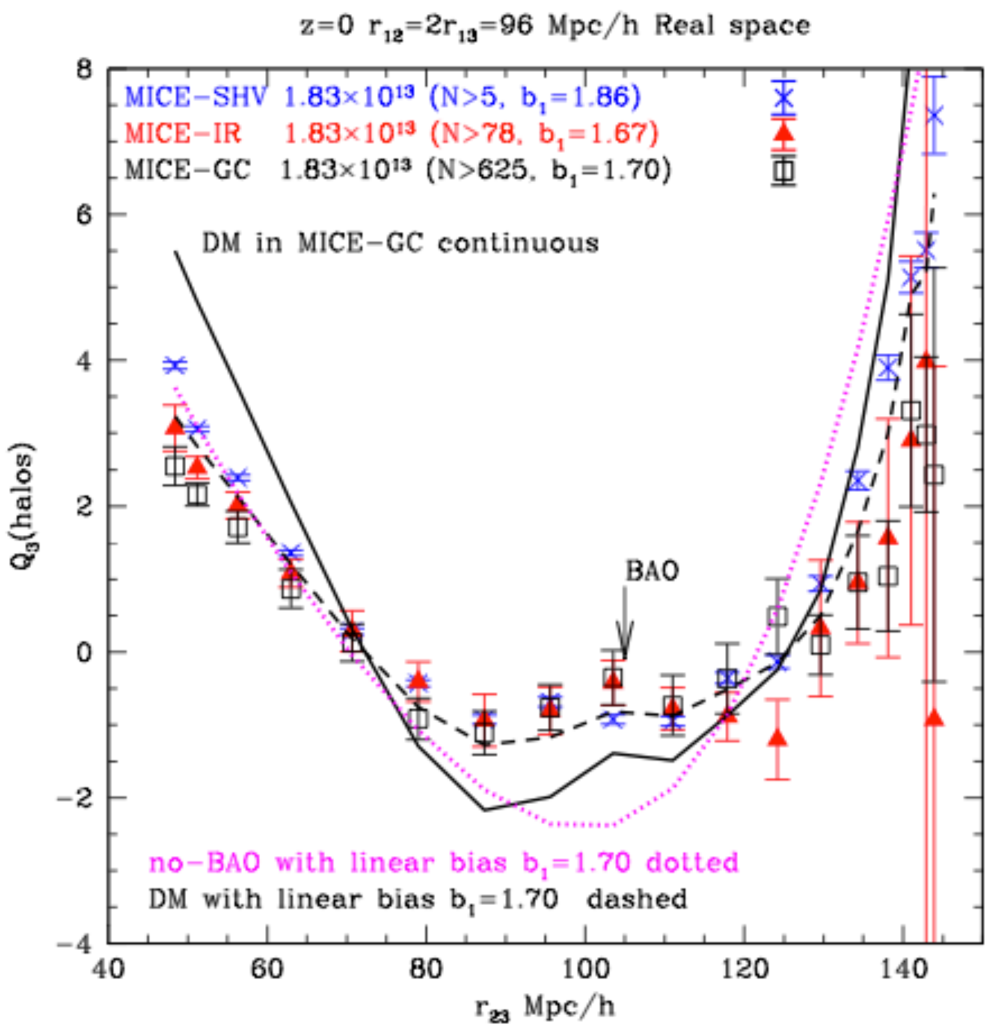

$$\xi^h(r) \simeq b_1^2\, \xi(r)$$

$$\zeta^h(r_{12}, r_{23}, r_{13}) \simeq b_1^3 \zeta(r_{12}, r_{23}, r_{13}) + + b_1^2 b_2 \left(\xi(r_{12})\xi(r_{13}) + \mathrm{cyc}\right)$$

$$Q_3^h \simeq \frac{1}{b_1}\,(Q_3 + c_2)$$

MICE-IR and MICE-GC show same differences as the 2-pt results (rather marginal for these halos).

Notice how Q_3 from MICE-SHV traces well the other measurements even with groups of 5 particles. However at the % level it fails.

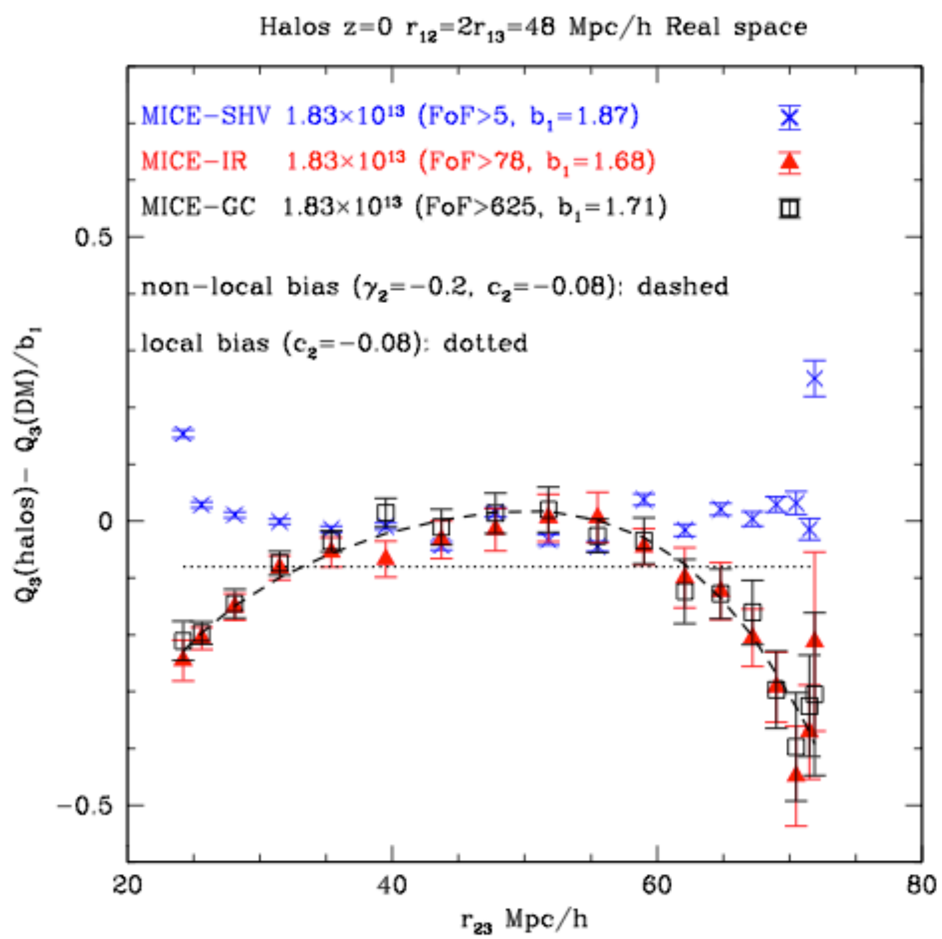

N-body simulations - limitations and things to be aware of

Force Tolerance

Size of mesh to go from grid to tree estimation of the forces

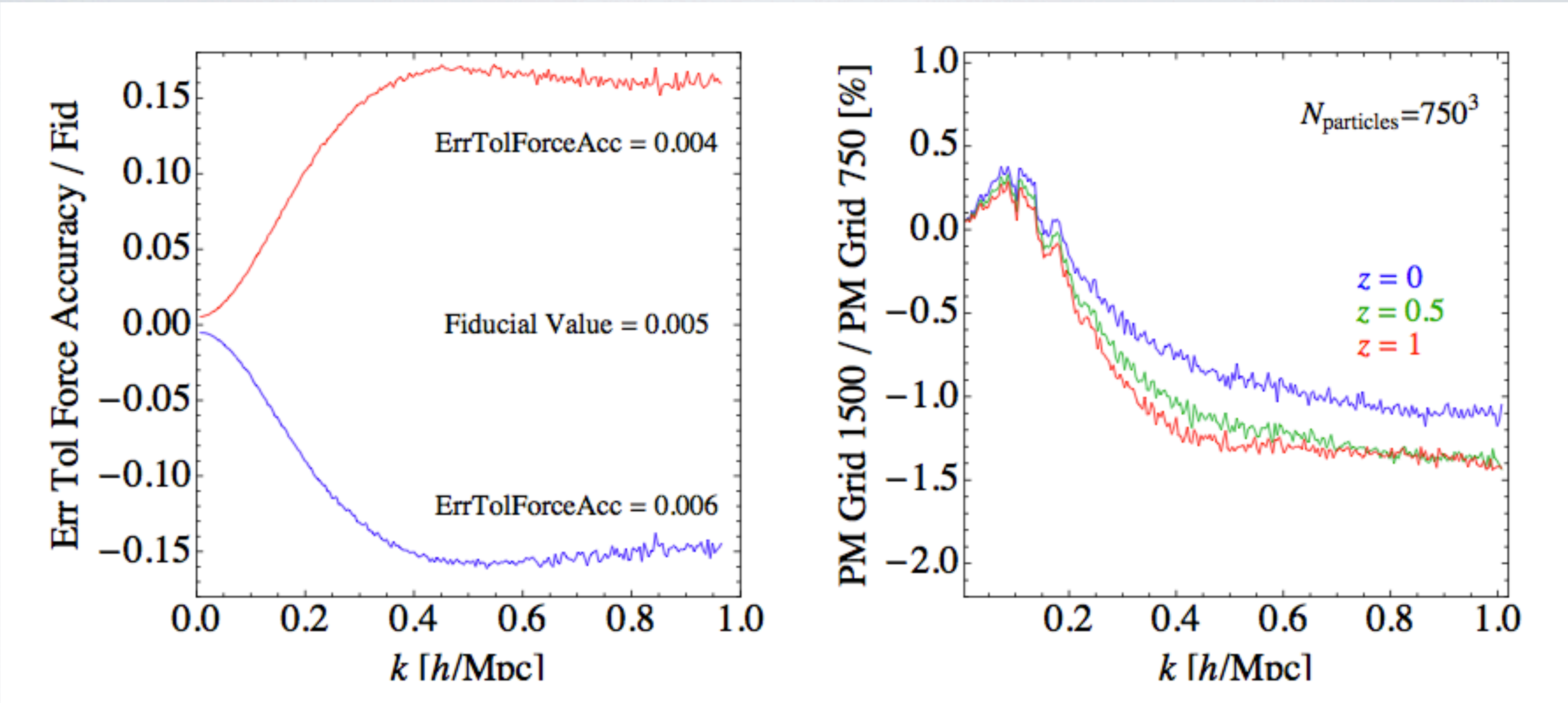

- The small scale physics is harder to capture and more sensible to simulation specifications, the large-scales seems safer but it all depends what you call nonlinear scale and the accuracy sought .. e.g. **k ~ 0.2 h/Mpc there will be % level effects from sim parameters.**

The MICE grand-challenge : halo and galaxy catalogs

- Built upon the MICE-Grand Challenge N-body simulation 70 billion particles with a DES-like volume (particle mass 3×10^{10} Msun/h)

Run	$N_{\rm part}$	$L_{\rm box}/\,h^{-1}\,{\rm Mpc}$	$PMGrid$	$m_p/(10^{10}\,h^{-1}\,{\rm M_\odot})$	$l_{\rm soft}/\,h^{-1}\,{\rm Kpc}$	$z_{\rm i}$	$Max.TimeStep$
MICE-GC	4096^3	3072	4096	2.93	50	100	0.02

- Full sky light-cone with minimal repetition up to z=1.4 + lensing maps

- More than 70 Million FoF(0.2) halos found on the LC (per octant) and 170 M at z=0

- We compute basic halo properties (center of mass, velocities) and store all dark matter particles belonging to each halo (allowing us to estimate shapes and angular momentum)

- Halo catalogue populated with galaxies using hybrid HOD + HAM techniques

Building the synthetic galaxy catalogue

Our goal is to model abundance and clustering across luminosity / color up to z ~ 1.4
We are not interesting in an HOD modeling of some preset galaxy type as typically done.

Using a hybrid Halo Occupation Distribution (HOD) and Halo Abundance Matching (HAM) technique we populate halos such as to match

- SDSS luminosity function at z=0.1 (Zehavi et al 2001)
- Clustering as a function of color and luminosity
- Color Distribution

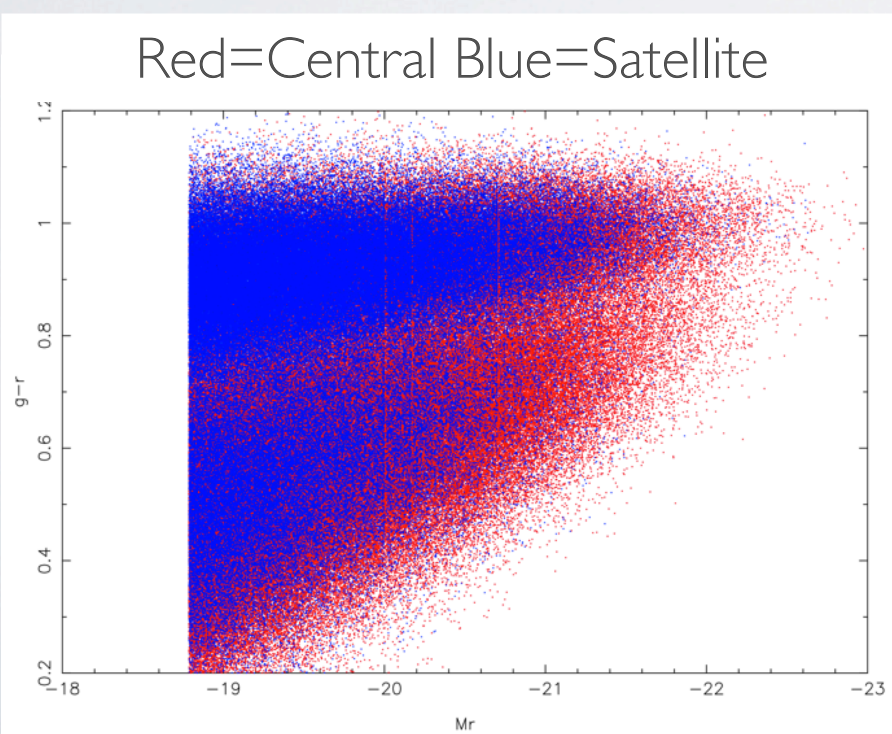

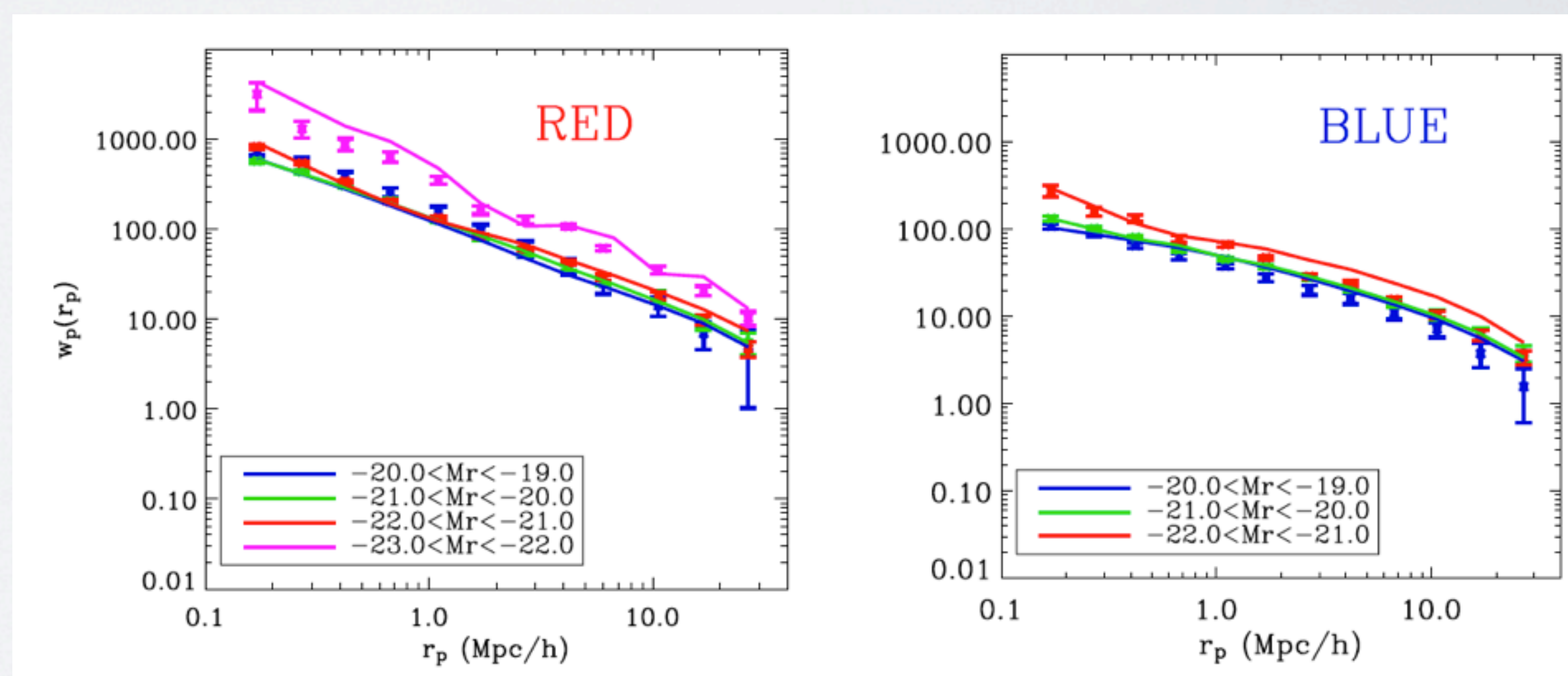

Building the synthetic galaxy catalogue

Our goal is to model abundance and clustering across luminosity / color up to z ~ 1.4
We are not interesting in an HOD modeling of some preset galaxy type as typically done.

Using a hybrid Halo Occupation Distribution (HOD) and Halo Abundance Matching (HAM) technique we populate halos such as to match

- SDSS luminosity function at z=0.1 (Zehavi et al 2001)
- Clustering as a function of color and luminosity
- Color Distribution

Once the fit works at lower redshift we use stellar population models to evolve galaxy properties to populate halos into the past light-cone.

Given luminosity and (g-r) color at a given redshift we sample a compatible full SED from the COSMOS catalogue (Ilbert et al 2009).

Validating galaxy properties and clustering in the light-cone

Predicted clustering in COSMOS

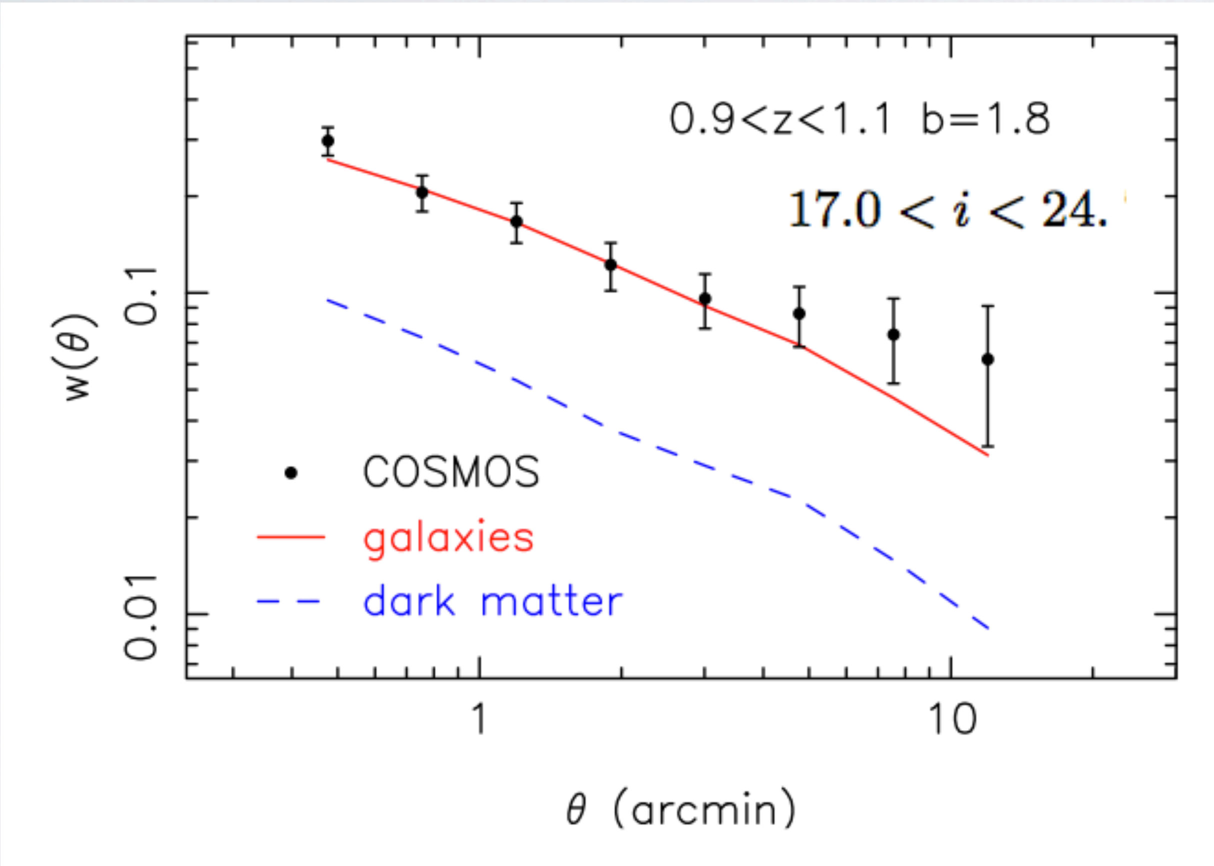

Distribution of colors

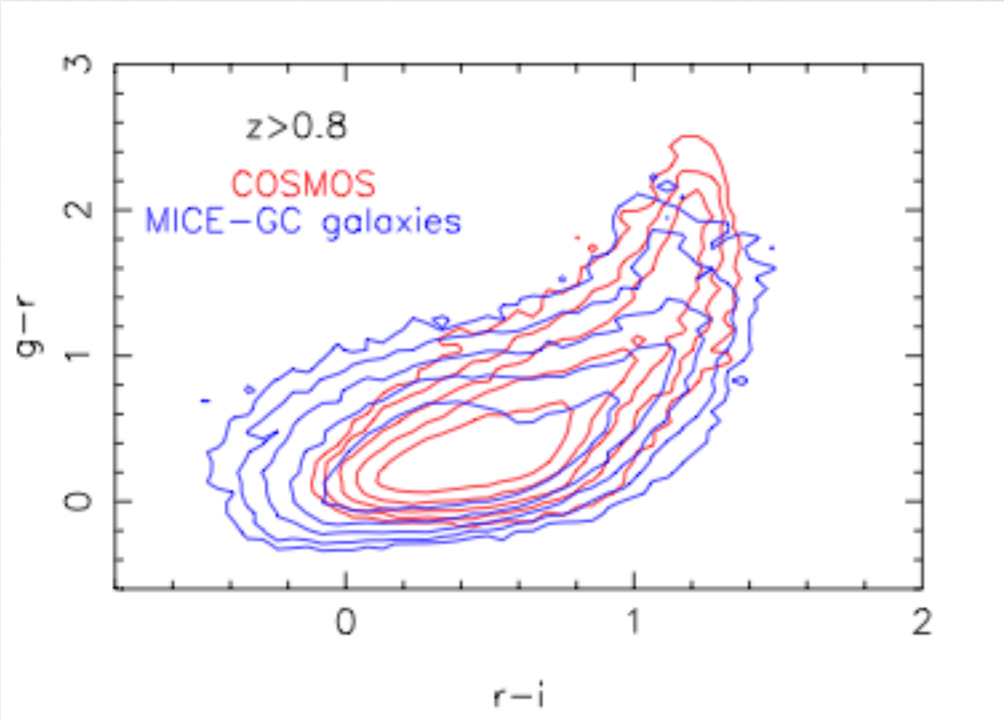

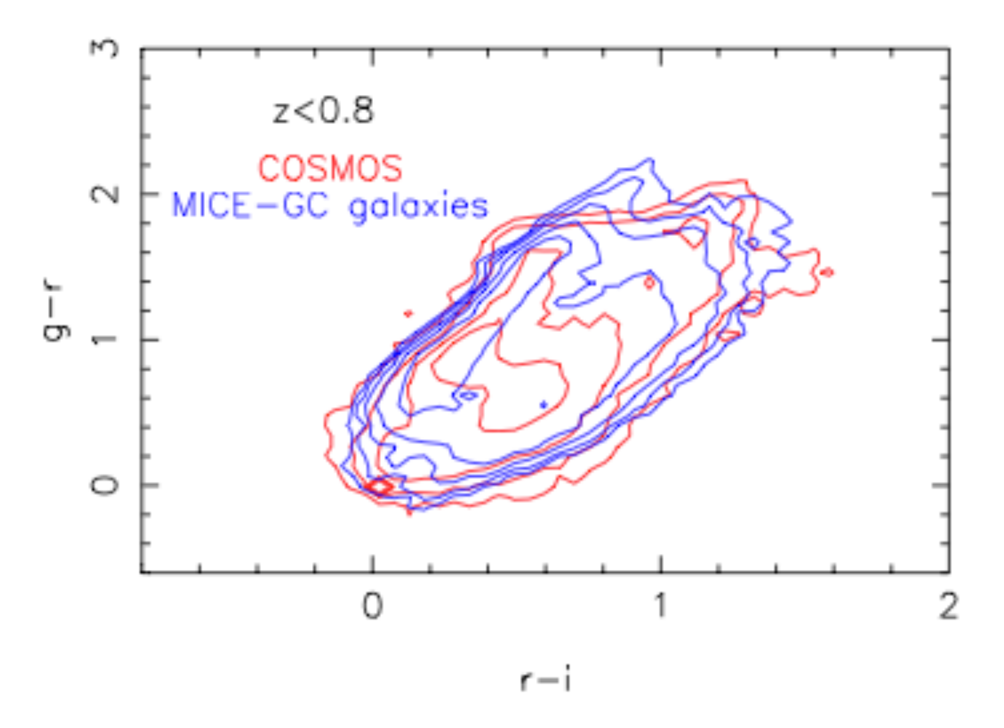

The MICE light-cone halo and galaxy catalog

Some basic numbers (for one octant of sky to z=1.4 equivalent to 3 Gpc/h away)

Mag Limit	N. of Galaxies	Sat. Fraction	$\langle M_h^{all} \rangle$	$\langle M_h^{cen} \rangle$	$M_{h,\min}^{cen}$	Red Cen. [%]	Red Sat. [%]
$M_r < -19$	1.92×10^8	0.23	1.0×10^{12}	6.35×10^{11}	2.23×10^{11}	35	77
$M_r < -20$	8.01×10^7	0.25	2.38×10^{12}	1.57×10^{12}	6.04×10^{11}	46	80
$M_r < -21$	1.42×10^7	0.24	8.29×10^{12}	6.74×10^{12}	1.94×10^{12}	62	87
$M_r < -22$	2.3×10^5	0.13	5.62×10^{13}	5.5×10^{13}	7.94×10^{12}	85	98

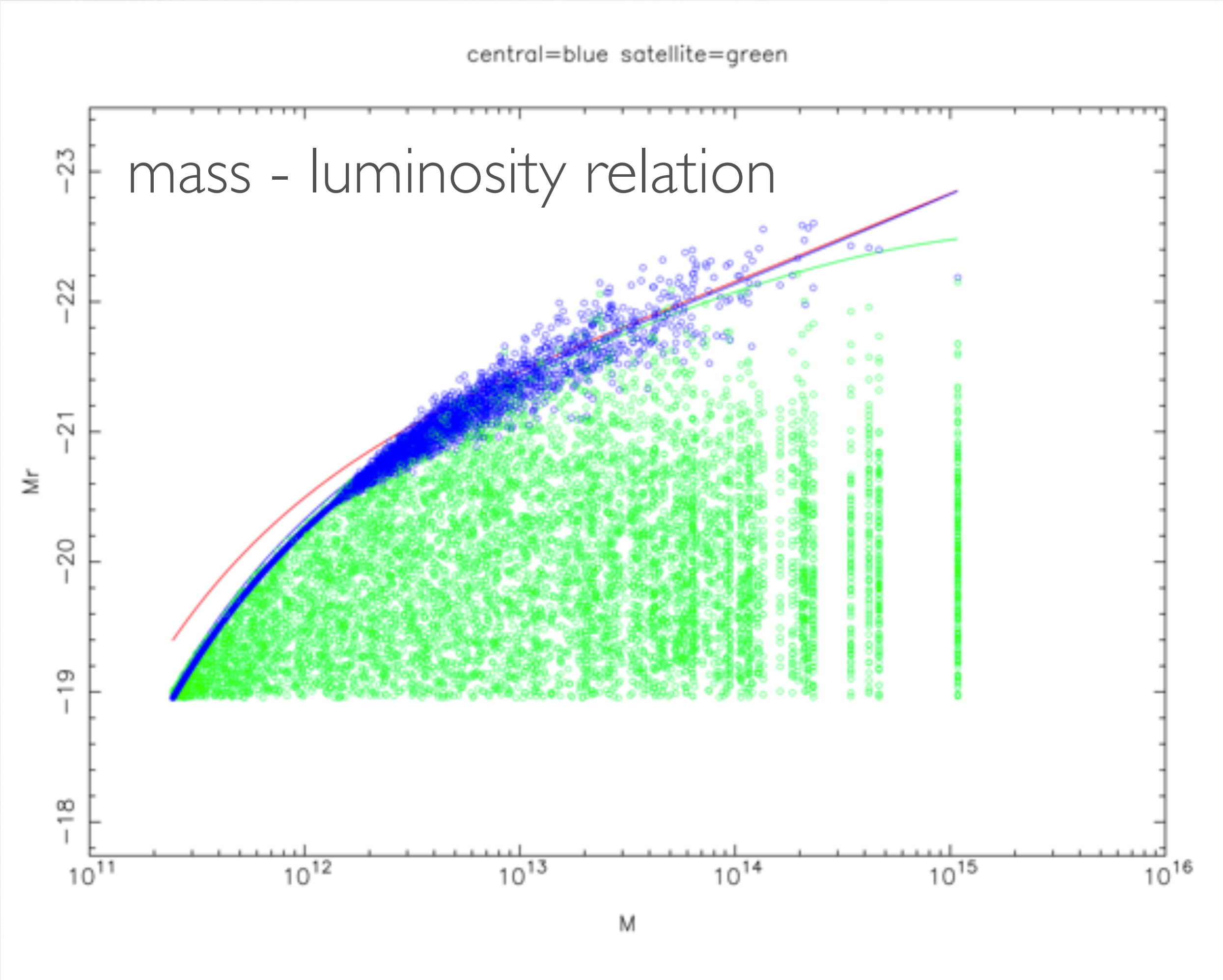

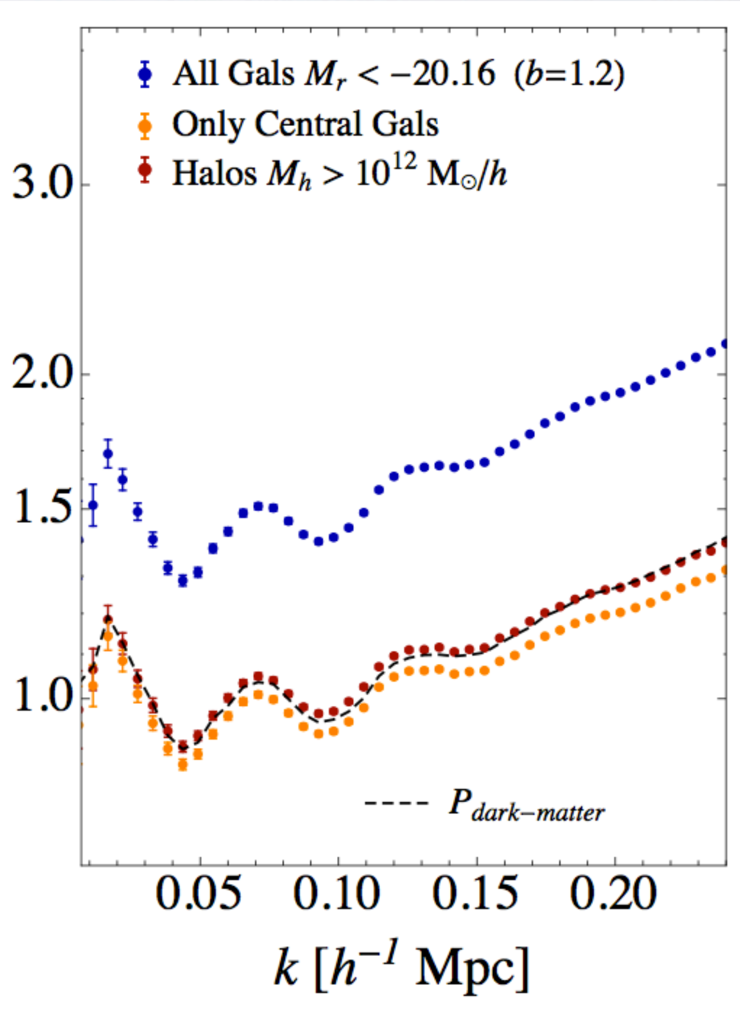

The MICE halo and galaxy catalog : Clustering

Halo Bias from small to large (BAO) scales

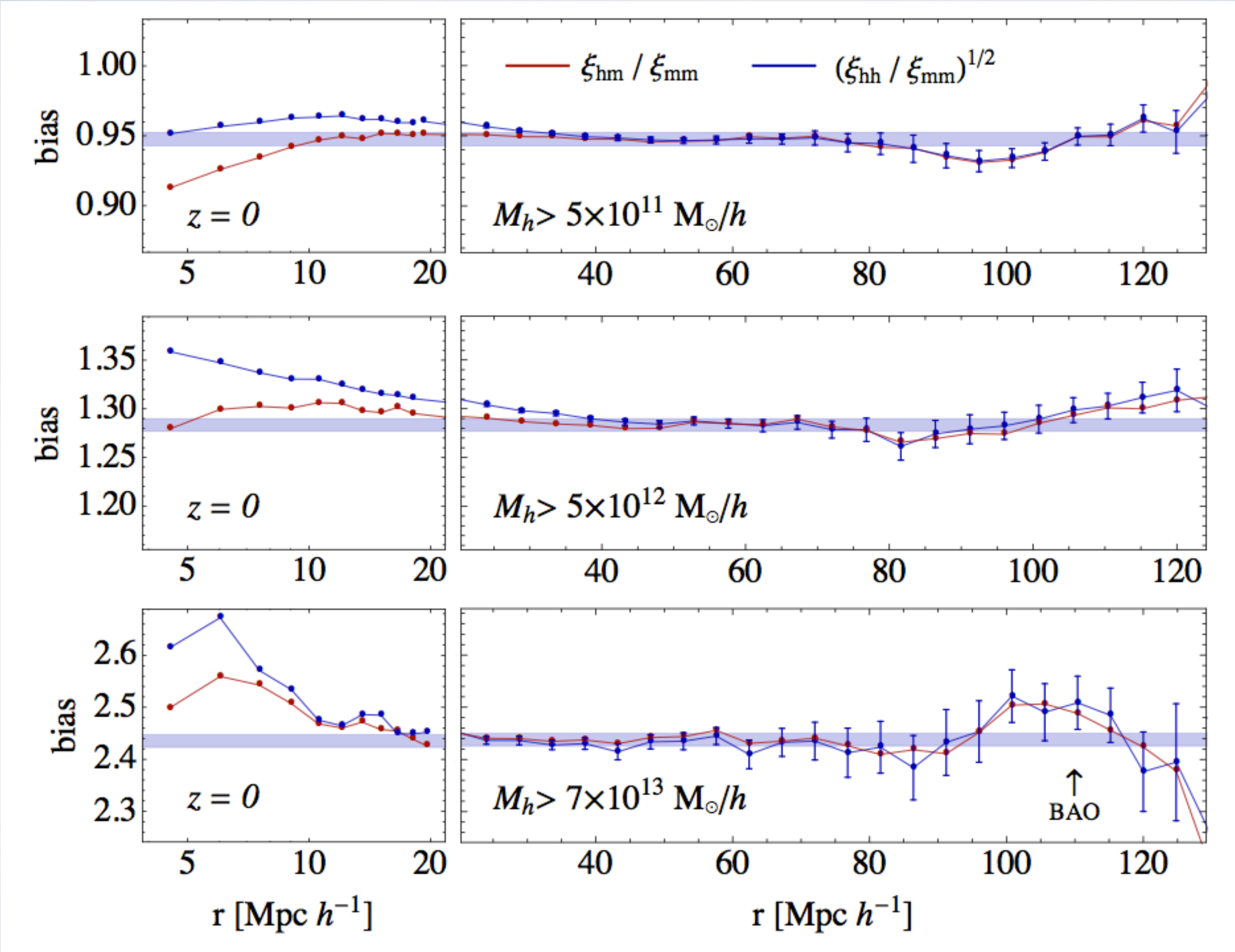

x-correlation coeff. departs from 1 at 20 Mpc/h

Bias is remarkably flat from small to large scales (few %) for Mstar halos

Excess clustering on BAO scales for massive objects

Galaxy Bias from small to large (BAO) scales

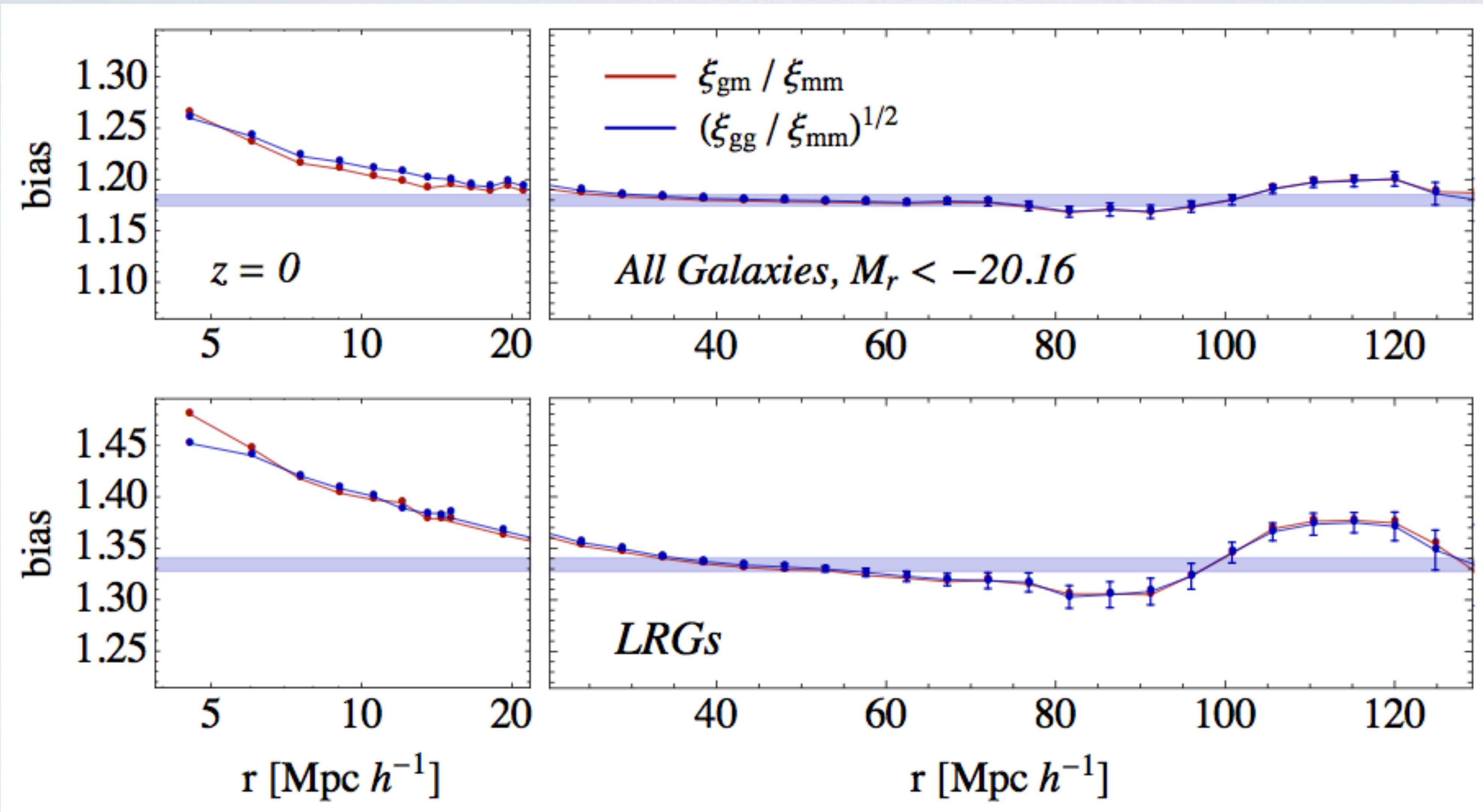

x-correlation coeff. stays close to unity

Bias is remarkably flat from small to large scales (few %) for Mr < 20

Excess clustering on BAO scales for most luminous objects

Here LRG are defined as Mr < -21 and (g-r) > 0.8 in rest frame colors

For LRG there is a tilt in the bias and ~ 6 % effects at BAO scales

Galaxy clustering in the light-cone at BAO scales

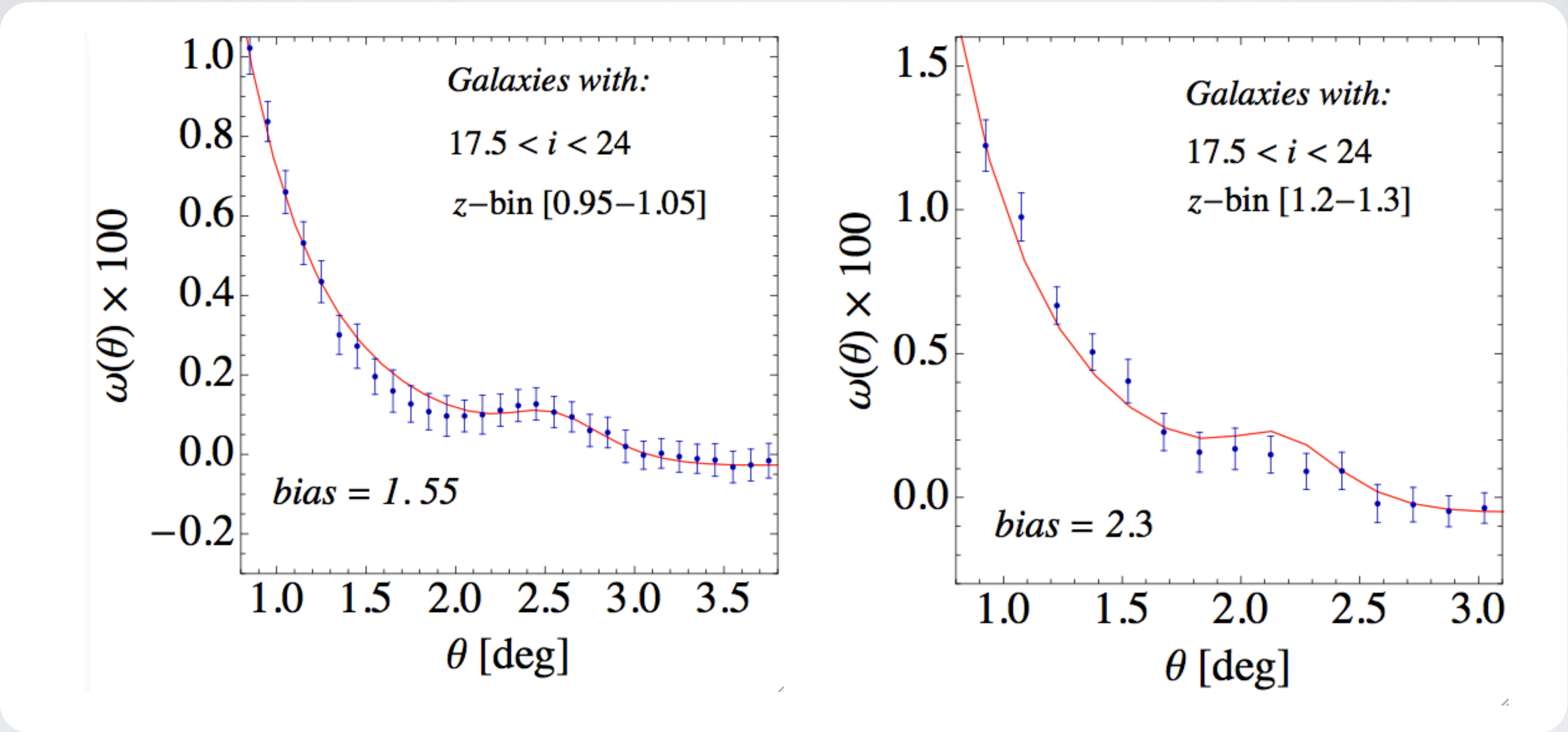

The MICE light-cone halo and galaxy catalog

validating galaxy velocities through RSD

Kaiser limit the LC : monopole

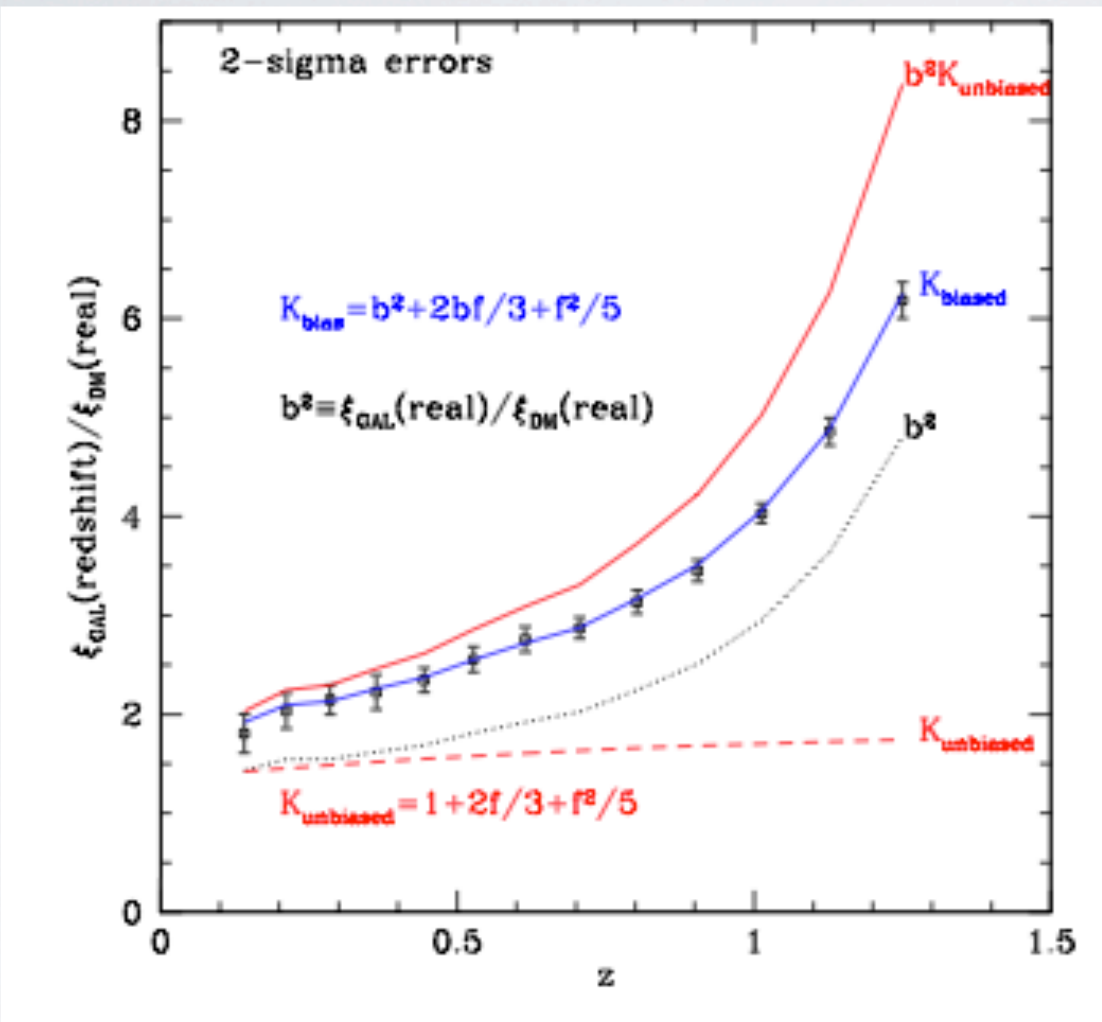

Impact of satellite virial motions

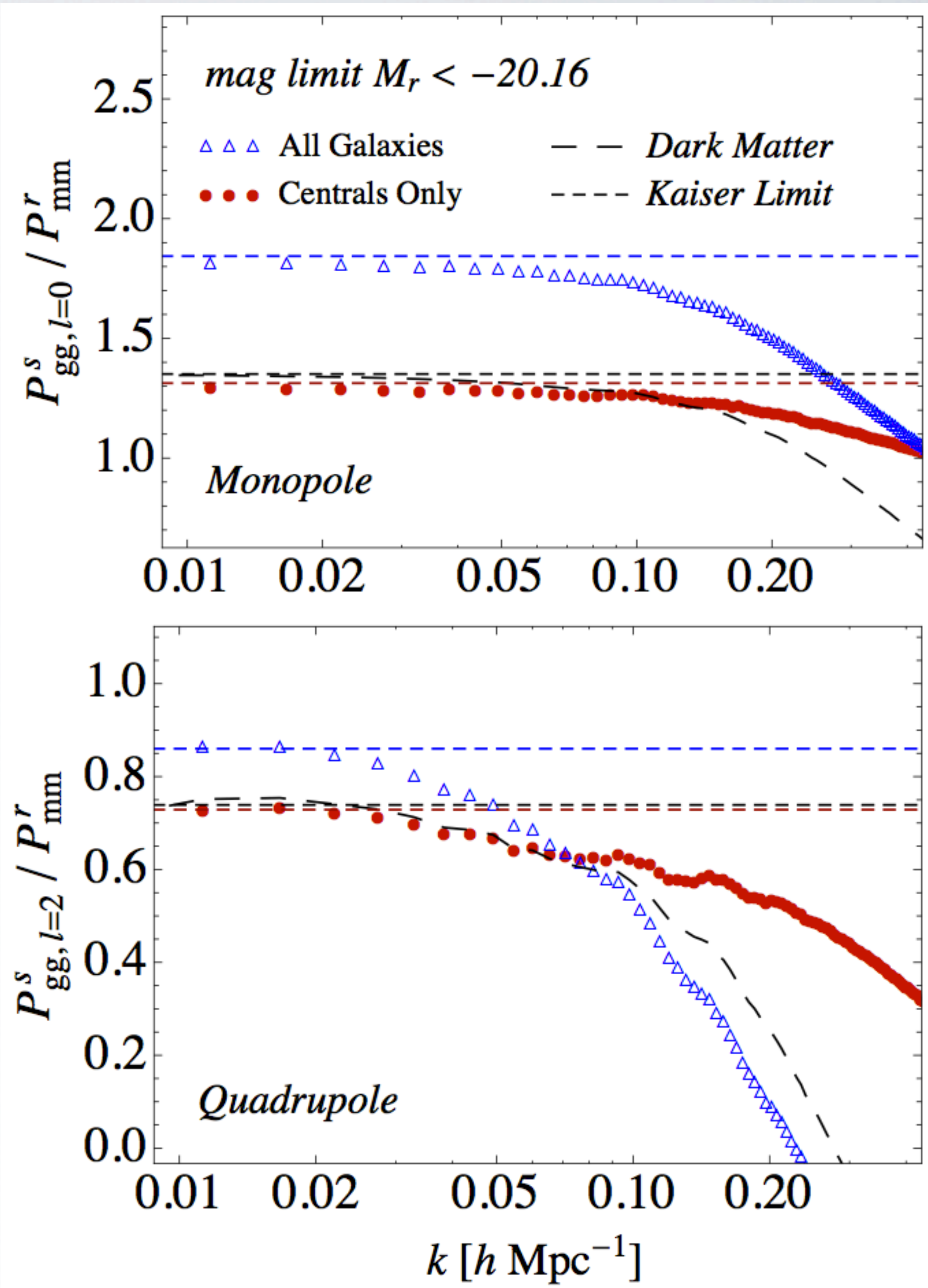

The MICE light-cone halo and galaxy catalog : full sky lensing maps

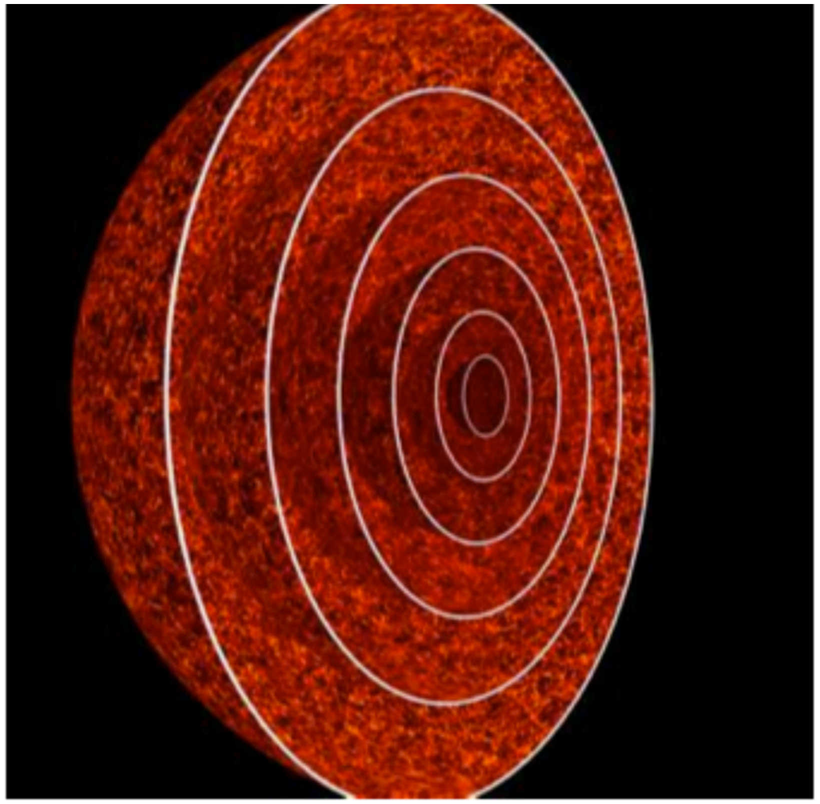

- Split the dark matter data into ~ 230 thin shells of width dz = 0.003(1+z)
- Interpolate densities into Healpix pixels with Nside = 4096 (pix resolution is 0.85 arc-min)
- Combine with appropriate lensing weight to produce convergence maps

$$\kappa(\theta) = \frac{3H_0^2\Omega_m}{2c^2} \int dr\ \delta(r,\theta) \frac{(r_s - r)r}{r_s\ a}$$

convergence field in each pixel

$$\kappa_i = \frac{3H_0^2\Omega_m}{2c^2} \sum_j \delta_{i,j} \frac{(r_s - r_j)r_j}{r_s a_j} dr_j$$

Born Approx.

From this it is then possible to obtain lensing potential $\kappa(\hat{\mathrm{n}}) = \nabla^2\phi(\hat{\mathrm{n}})$ and hence many other lensing observables such as shear, magnification, flexion etc.
Having full sky simplifies life a lot !

The MICE light-cone lensing maps : convergence and deflection angle spectra

$$C_\ell(\kappa) = \frac{9H_0^4\Omega_m^2}{4c^4} \int dr\ P(k,z)\frac{(r_s-r)^2}{r_s^2\ a^2}$$

$$\alpha(\hat{n}) = \nabla\phi(\hat{n})$$

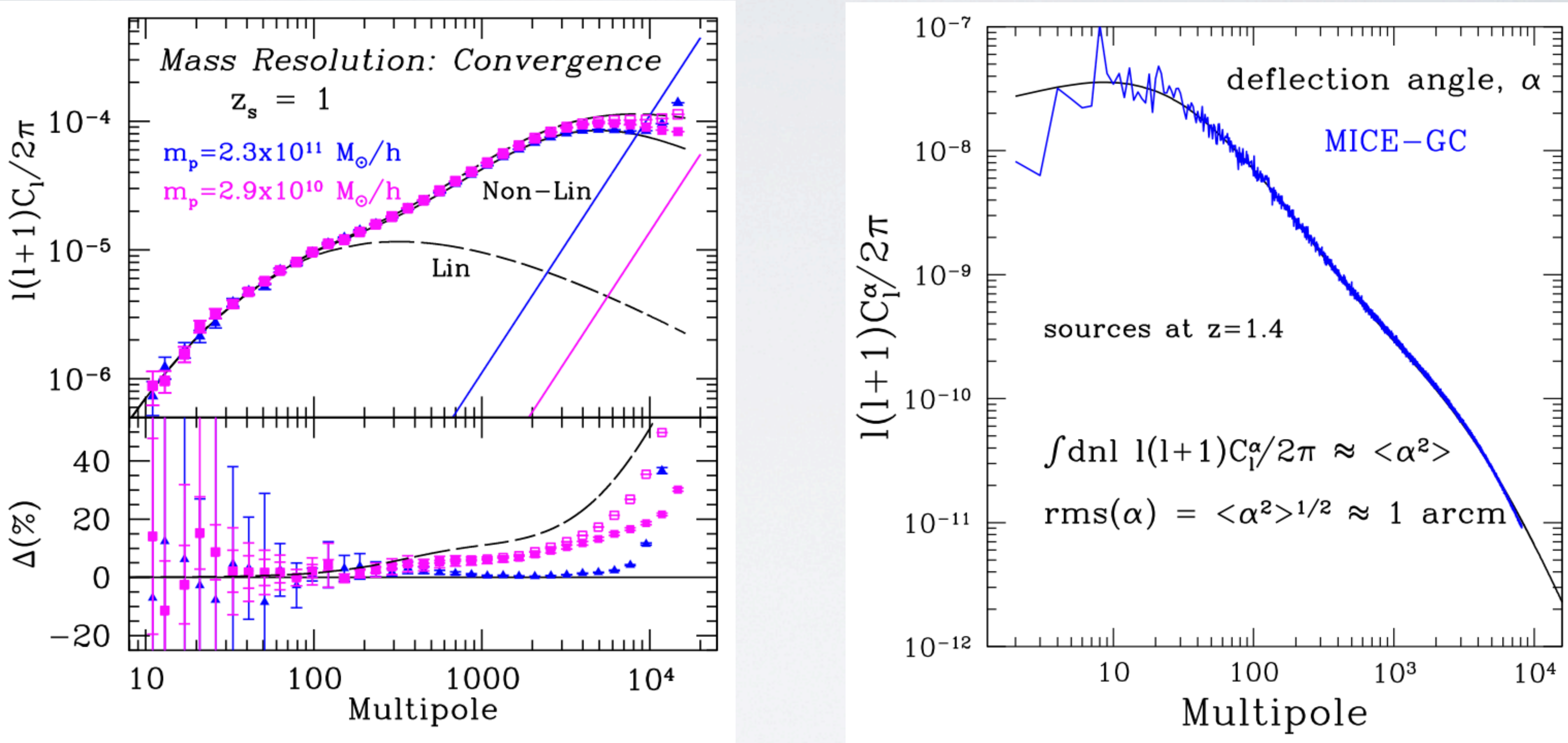

Mass resolution in convergence are at 5% for $l \sim 10^3$ and 20% at $l \sim 10^4$

The agreement with Halofit 2012 is at the 5% level at $l \sim 10^3$

The MICE light-cone lensing maps : Galaxy Lensing cross correlations

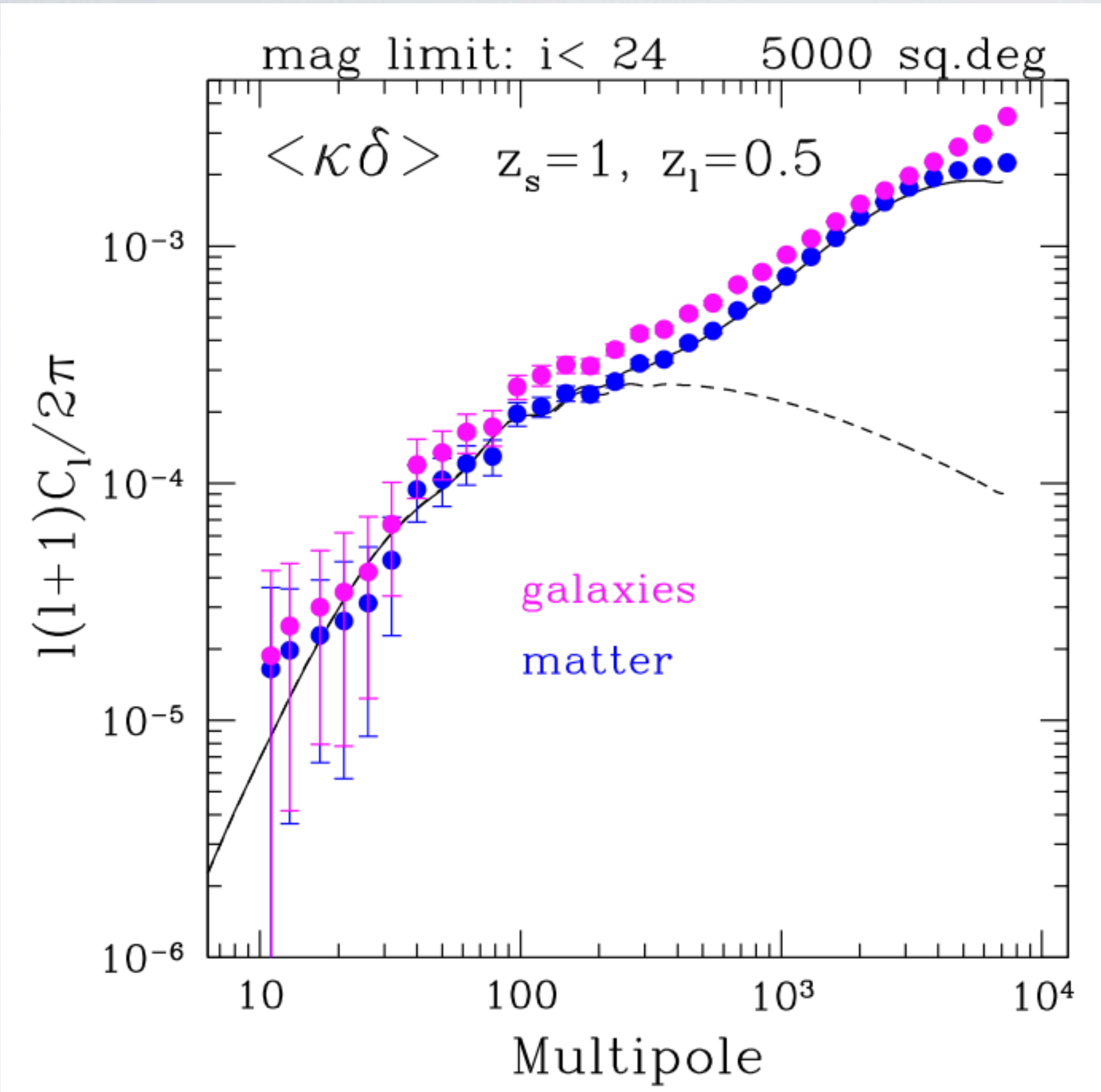

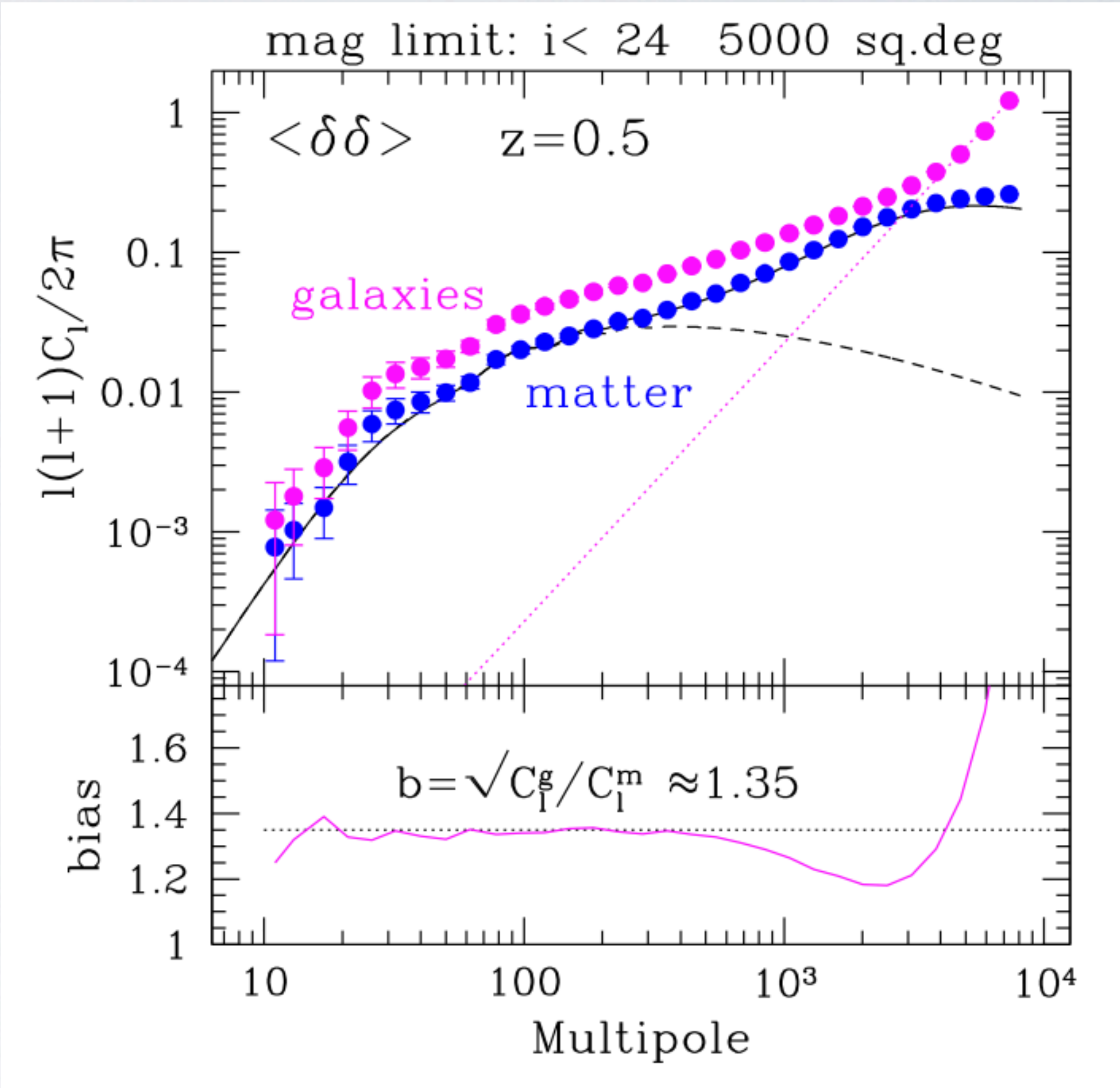

Cross-correlation of source (z~1) convergence field with lenses (z ~ 0.5).

This is expected to depend only in the bias of background population

The MICE light-cone lensing maps : Galaxy Lensing

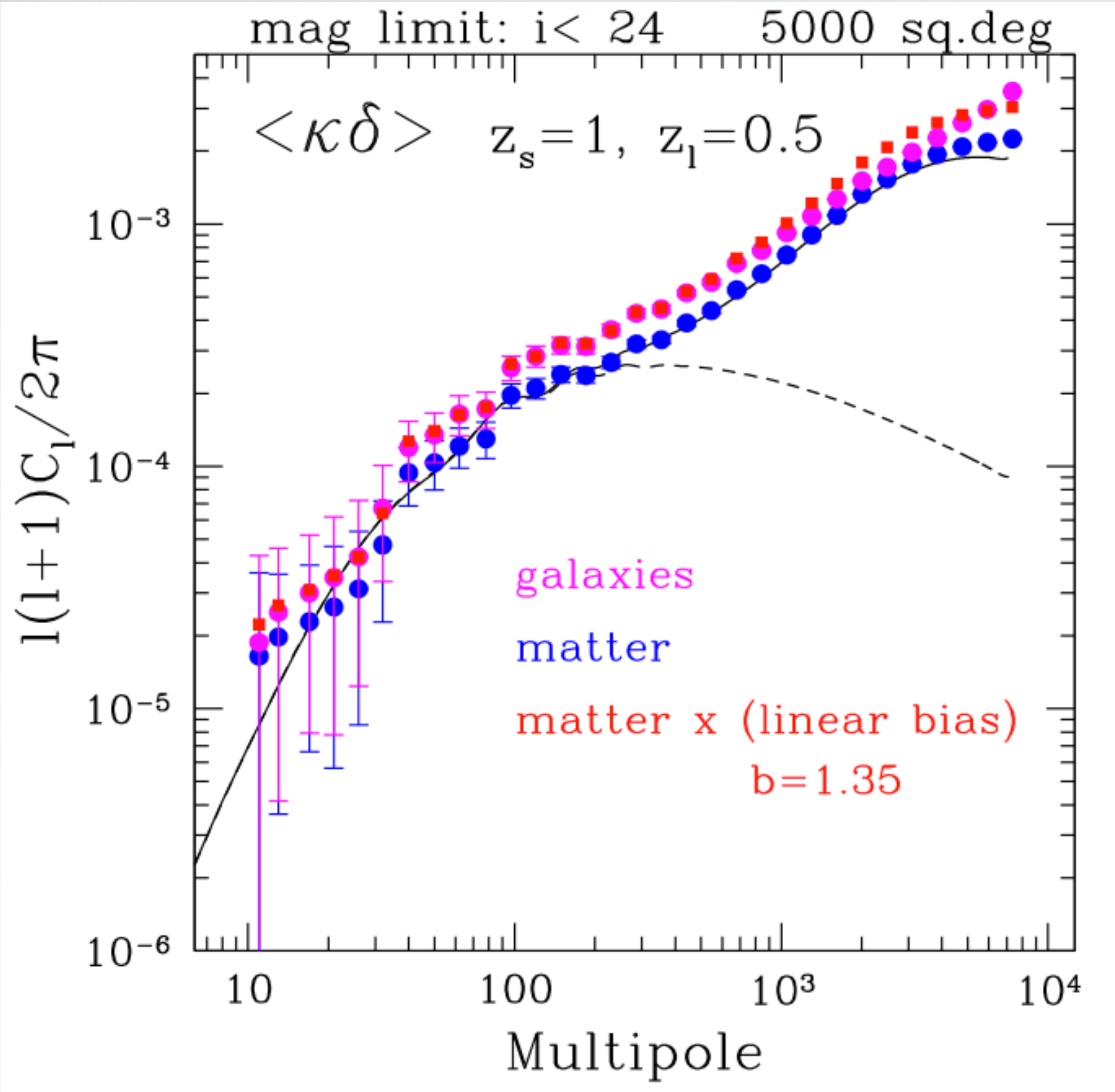

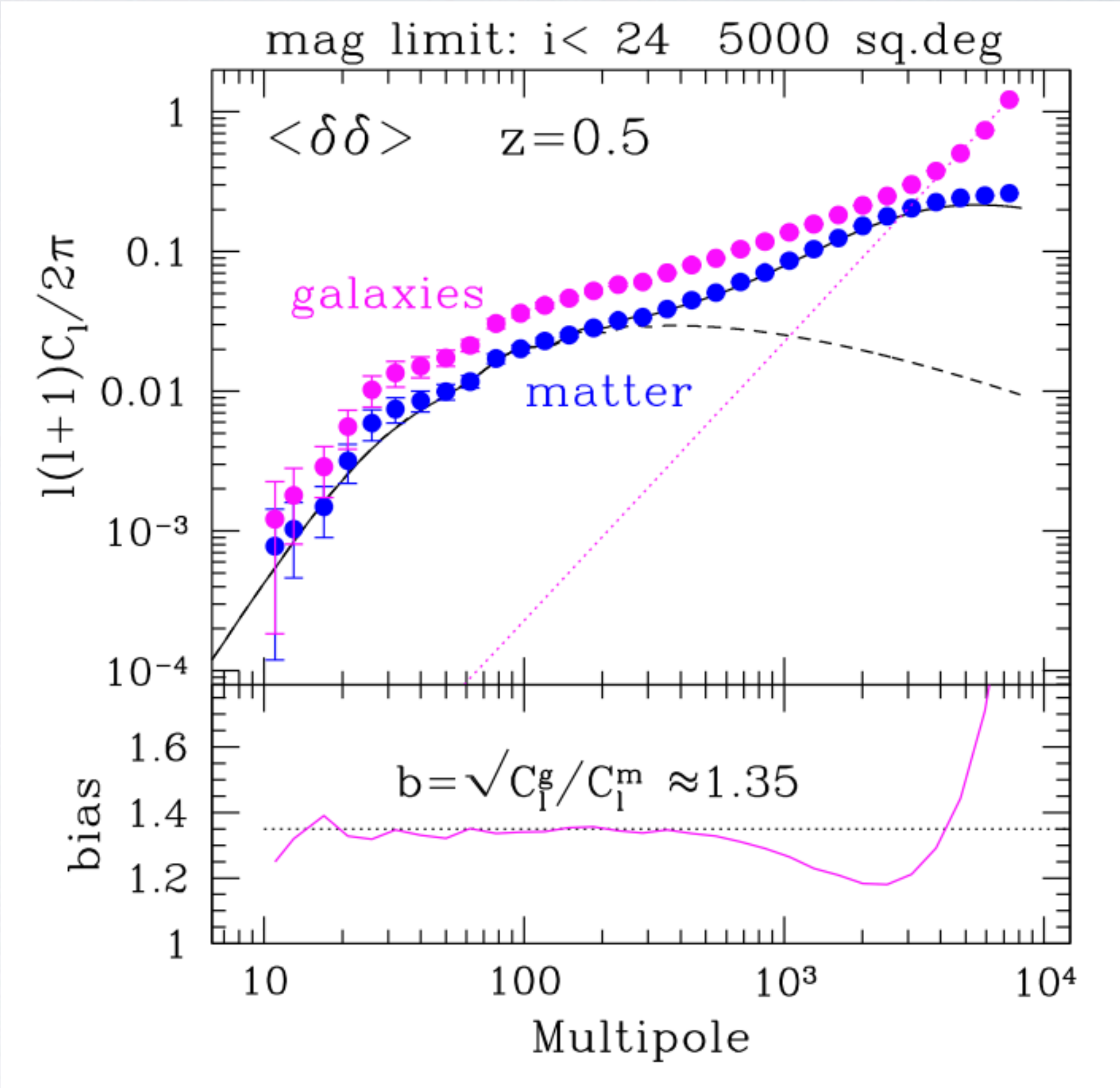

Cross-correlation of source (z~1) convergence field with lenses (z ~ 0.5).

This is expected to depend only in the bias of background population

This is indeed what we find (shown in right panel b = 1.35)

The MICE light-cone lensing maps : Lensing Magnification

Lensing increases the observed depth (flux limit) and increases the effective survey area (preserving surface brightness) $f \to f/\mu,$ $A \to A/\mu,$

Cumulative number count above a flux limit f scales as $N_0(>f) \sim A f^{\alpha},$

Hence we have *magnification bias* $$N(>f) \sim \frac{1}{\mu} A \left(\frac{f}{\mu}\right)^{-\alpha} = \mu^{\alpha-1} N_0(>f)$$

In the weak lensing limit $\mu = 1 + \delta_\mu$ $\delta_\mu = 2\,\delta_\kappa$

Magnified over-densities of background sources is given by

$$\begin{aligned} \delta_{all} &= \frac{N - N_0}{N_0} = \delta_m + \delta_p \\ &= (\alpha - 1)\delta_\mu = (2.5s - 1)\delta_\mu = (5s - 2)\delta_\kappa \end{aligned}$$

$$s = 2\alpha/5 \equiv \frac{d\mathrm{Log}_{10} N(<m, z)}{dm}.$$

slope of back-ground number count at mag limit

2 effects

(i) *magnified magnitudes,* $\delta_m = \alpha\delta_\mu,$
(ii) *magnified or lensed positions,* $\delta_p = -\delta_\mu.$

The MICE light-cone lensing maps : Lensing Magnification

We have added magnified positions and magnified magnitudes to the galaxies in our mock catalogue given the deflection angle and the magnification pixel value.

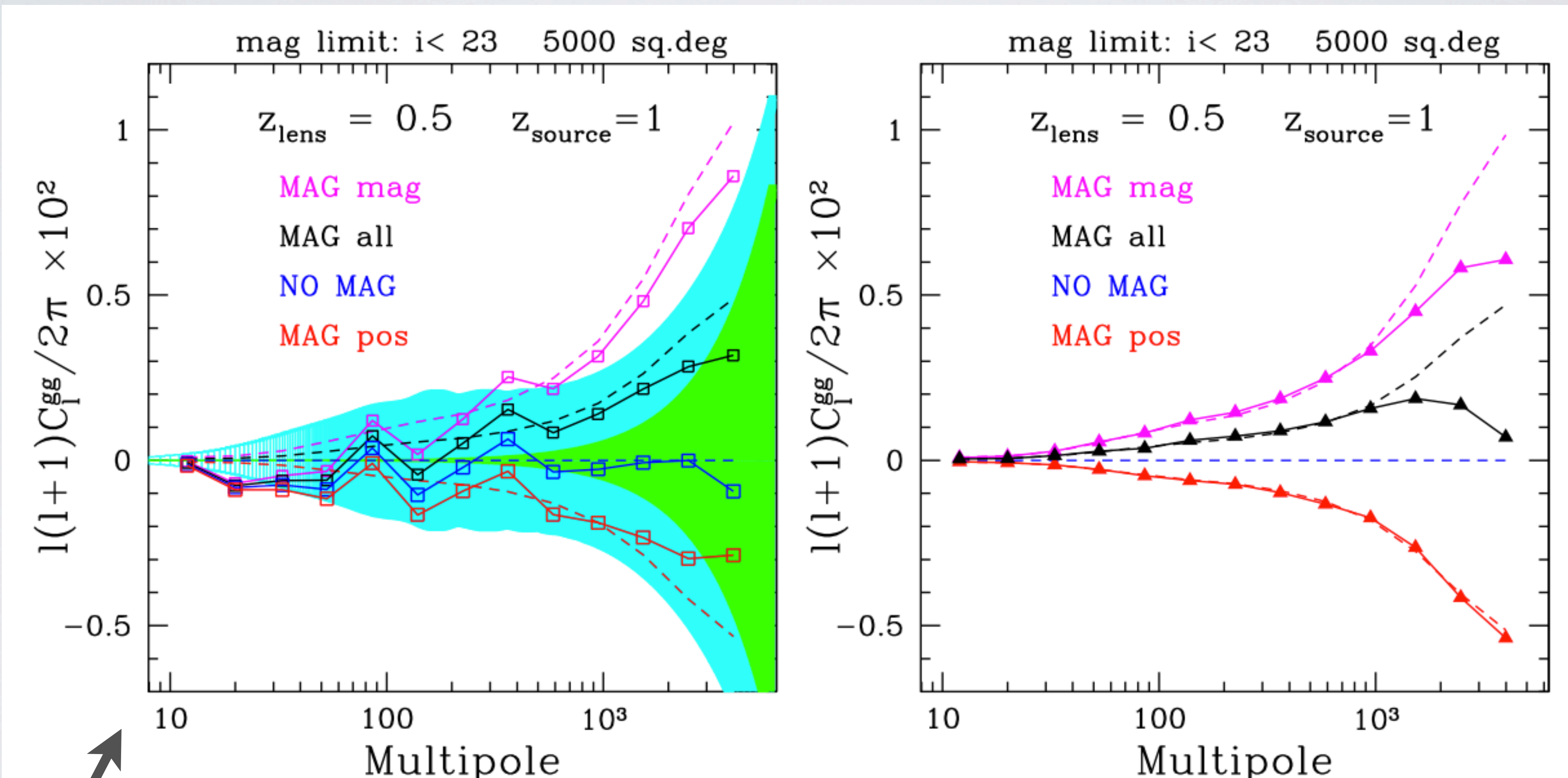

$< \delta(z_l)\delta_{mag}(z_s) >$	MAG mag,
$< \delta(z_l)\delta_{pos}(z_s) >$	MAG pos,
$< \delta(z_l)\delta_{all}(z_s) >$	MAG all,
$< \delta(z_l)\delta_{nomag}(z_s) >$	NO MAG,

- The magnification signal (which for this case is noise dominated b/c it a single pair) is very consistent with NL predictions down to pix resolution

The MICE light-cone halo and galaxy public catalog

MICE-GC Light-cone Galaxy Catalogues release

Catalogues include

- Positions RA, DEC
- Observed and true redshift
- Host halo mass
- Flags for central / satellite distinction
- Galaxy velocities (bulk + virial motion)
- Magnitudes in multiple bands (SDSS, DES, Euclid)
- Lensing information (convergence shear, magnification in pos and mag)
- Photo-z

next round -- galaxy sizes and shapes, intrinsic alignments

http://cosmohub.pic.es

The MICE light-cone halo and galaxy public catalog

http://cosmohub.pic.es

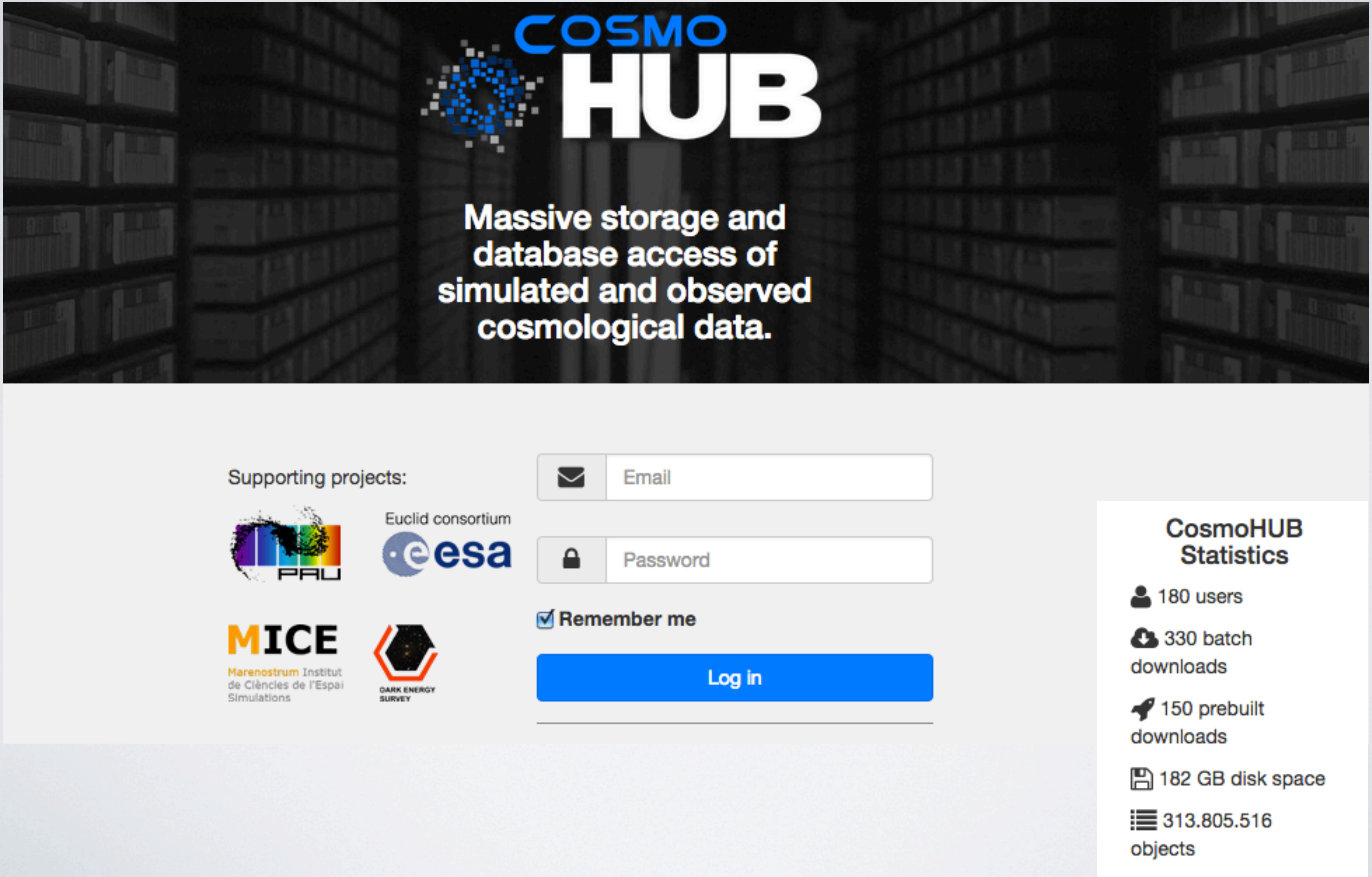

The MICE light-cone halo and galaxy public catalog

Value-Added Data | Custom Catalogs

Step 1: Select Fields

Check All | Uncheck All

- **id** object id
- **ra** right ascension (degree)
- **dec** declination (degree)
- **ra_mag** magnified right ascension (degree)
- **dec_mag** magnified declination (degree)
- **z** true redshift
- **zb** most likely redshift (output from the BCNZ code IS a modified version of the photo-z template based code BPZ developed by Benitez 2000)
- **odds** likelihood that z_b is correct (within 0.10) (output from the BCNZ code IS a modified version of the photo-z template based code BPZ developed by Benitez 2000)
- **log_m** log base 10 of FoF halo mass using Warren correction
- **abs_mag_r** absolute magnitude including evolution (Mr-5log(h))
- **g_des_realization** realization of g_des
- **g_des_realization_error** error of the realization of g_des
- **r_des_realization** realization of r_des
- **r_des_realization_error** error of the realization of r_des
- **i_des_realization** realization of i_des
- **i_des_realization_error** error of the realization of i_des
- **z_des_realization** realization of z_des
- **z_des_realization_error** error of the realization of z_des
- **y_des_realization** realization of y_des
- **y_des_realization_error** error of the realization of y_des
- **j_vhs_realization** realization of j_vhs
- **j_vhs_realization_error** error of the realization of j_vhs
- **h_vhs_realization** realization of h_vhs
- **h_vhs_realization_error** error of the realization of h_vhs
- **ks_vhs_realization** realization of ks_vhs
- **ks_vhs_realization_error** error of the realization of ks_vhs
- **kappa** convergence
- **gamma1** shear
- **gamma2** shear

The MICE light-cone halo and galaxy public catalog

Step 2 (optional): Apply filters

z | < | 0.5

Add Filter

Step 3 (optional): Customize the SQL query

```
SELECT id,ra,dec,ra_mag,dec_mag,z,zb,odds,log_m,abs_mag_r,g_des_realization,g_des_realization_error,r_des_realization
,r_des_realization_error,i_des_realization,i_des_realization_error,z_des_realization,z_des_realization_error,y_des_reali
zation,y_des_realization_error,j_vhs_realization,j_vhs_realization_error,h_vhs_realization,h_vhs_realization_error
,ks_vhs_realization,ks_vhs_realization_error,kappa,gamma1,gamma2
 FROM des_mice_v0_4_r1_4_view
 WHERE  z < 0.5
```

Step 4: Check & Run

QUERY has been succesfully checked.

Estimated number of rows: ~6.84e+7

Estimated size: ~10.1 GB

Plot & Preview

Run Query

Summary

- Standard PT can be turned into a practical tool satisfying current survey requirements

I introduce the MICE grand challenge end-to-end simulation, discussed the dm the halos and the HOD+SAM galaxies catalogue

- Large Scale BAO clustering agrees very well with PT and <2% with numerical fits.

- The agreement with fits towards smaller scales is within 5% in a set of different observables

- Particle mass resolution effects can be relevant at the 5%-10% level or more depending on scale and observable. Run with 10e12 particle mass show larger differences

- Scale Dependence of bias in both halo and galaxies. Few % effect for LRGs and massive halos at BAO region.

- We discuss how to paint lensing properties to galaxies, in particular magnification

- The MICE-GC Light-cone Halo and Galaxy Catalogues available at

`http://catalog.astro.pic.es`